International Journal of Automotive Technology, Vol. 21, No. 6, pp. 1597–1618 (2020)
DOI 10.1007/s12239–020–0150–4

pISSN 1229–9138/ eISSN 1976–3832

REVIEW OF RECENT AFTER-TREATMENT TECHNOLOGIES FOR DE-NOx PROCESS IN DIESEL ENGINES

Byungchul Choi[1, 2)*], Kyungseok Lee[2, 3)] and Geonseog Son[4)]

[1)]School of Mechanical Engineering, Chonnam National University, Gwangju 61186, Republic of Korea
[2)]Automotive Research Center, Chonnam National University, Gwangju 61186, Republic of Korea
[3)]University Industry Liaison Office, Chonnam National University, Gwangju 61186, Republic of Korea
[4)]Umicore Korea, 71-3 Gongdan 2ro, Seobuk-gu, Cheonan-si 31093, Republic of Korea

(Received 25 September 2020; Revised 17 October 2020; Accepted 17 October 2020)

ABSTRACT–The removal of nitrogen oxides (NOx), which are major atmospheric pollutants, in exhaust gas after-treatment systems, has been studied extensively. The catalytic reduction of NOx in lean-burn environments is challenging in diesel after-treatment technology. The most relevant catalytic NOx reduction technologies for diesel engines are summarized in this review paper, focusing on current catalytic after-treatment systems for compliance with emission standards. Four promising after-treatment technologies for the abatement of tail-pipe NOx emissions are discussed: (i) lean NOx trap (LNT) and LNT combined with selective catalytic reduction (SCR) (LNT + SCR), (ii) Urea/NH_3-SCR, (iii) Hydrocarbon-SCR (HC-SCR), and (iv) CO/H_2-SCR. The relevant reaction mechanisms and current major challenges are reviewed in detail. The effects of the active phases and support modifications of the respective catalysts are examined to evaluate their contribution to the after-treatment systems. Major issues in practical applications, such as hydrothermal aging, chemical poison, and metallic additives for improving de-NOx performance, are extensively reviewed in this paper.

KEY WORDS : Diesel engine, After-treatment, Catalyst, De-NOx, LNT, SCR

NOMENCLATURE

AIE : aqueous ion exchange
CDPF : catalyzed diesel particulate filter
CeO_2 : ceria
CHA : chabazite
CVD : chemical vapour deposition
DME : dimethyl ether
DOC : diesel oxidation catalyst
DPF : diesel particulate filter
HC : hydrocarbon
HNCO: isocyanic acid
LNT : lean NOx trap
LOT : light-off temperature
NH_3 : ammonia
NOx : nitrogen oxide
NSC : NOx storage capacity
PGM : precious group metal
PM : particulate matter
RDE : real driving emission
SCR : selective catalytic reduction
SDPF : SCR-catalyzed diesel particulate filter
SR : steam reforming
SSIE : solie-state ion exchange
TWC : three-way catalyst
UHC : unburned hydrocarbon
WGS : water-gas shift

*Corresponding author. e-mail: bcchoi@chonnam.ac.kr

1. INTRODUCTION

Currently, emission reduction and fuel economy improvement are two key challenges in the use of diesel engines. Emission reduction focuses on the problem of nitrogen oxides (NOx) and particulate matter (PM) emissions. Extremely reduced NOx emissions are required to meet current and future emission regulations such as California LEV-III, US Tier 3, and Euro 7. Particularly, the importance of real driving emission (RDE) was emphasized after the VW diesel gate scandal. After-treatment technologies such as selective catalytic reduction (SCR) or the lean NOx trap (LNT) are required in diesel vehicles to achieve these low levels of emissions.

The LNT is a promising de-NOx technology. Its system uses a catalyst consisting of a storage material and precious group metals (PGMs) with an γ-alumina wash coat. The reaction of the LNT catalyst occurs in lean to rich cycles. NO is adsorbed onto the storage materials and oxidized to NO_2 over the PM catalyst and stored on the surface in nitrate form. In the rich cycle, the stored NO_2 is released from the catalyst surface and reduced to N_2 by

hydrocarbons (HCs), CO, and H_2, which are intermediate components formed from the combustion of fuels over the PM catalysts (Praveena and Martin, 2018). The LNT catalyst was first proposed by Takahashi *et al*. (1996). Since then, this technology has been developed for 25 years and is being applied in automobile after-treatment systems. The LNT method offers low-temperature activity by adsorbing NOx, but is limited at high temperatures. However, the LNT catalyst has two major performance degradation issues, namely, sulfur poisoning and thermal aging.

SCR is a method of converting NOx into N_2 and H_2O, with the aid of a catalyst. Ammonia or urea solution is added to a fuel stream or exhaust gas as a reductant and is adsorbed onto the catalyst. CO_2 is produced as the reaction ends. The SCR of NOx using ammonia as the reducing agent was patented in the United States by the Engelhard Co. in 1957. The development of SCR technology continued in Japan and the US in the early 1960s, with research focusing on less expensive and more durable catalyst agents. The use of SCR systems in automobiles began approximately two decades ago (Tschoeke *et al*., 2010; Koebel *et al*., 1996; Schaber *et al*., 1999). The SCR method is suitable for heavy-duty diesel vehicles because of its higher NOx reduction potential. In this paper, we review the current status of LNT and SCR technologies for the de-NOx process among diesel engine vehicle after-treatment technologies.

2. LNT TECHNOLOGY

2.1. Reaction Mechanism

During the (longer) lean phase (O_2 in excess, several minutes), NOx are adsorbed on the storage sites (typically Ba^{2+}) in the form of nitrites and nitrates (reaction (1)). When the storage capacity of the catalyst is saturated, the rich phase (fuel in excess, several seconds) is triggered and the previously stored NOx are released and reduced to N_2 mainly, with traces of N_2O and/or NH_3 (reactions (2 ~ 4)). This allows the regeneration of the catalyst and availability to store more NOx under lean conditions (Takahashi *et al*., 1996; Roy and Baiker, 2009). Typically, the LNT catalyst contains storage materials (e.g. $BaO(CO_3)$, CeO_2), support materials (e.g. Al_2O_3 and CeZrOx), and PGMs (e.g. Pt, Pd, and Rh). Pt and Pd mainly oxidize NO, whereas Rh is used to reduce NOx. The NOx storage and oxidation sites are usually in close proximity (Vaclavik *et al*., 2016).

$$BaO + 3NO_2 \rightarrow Ba(NO_3)_2 + NO \quad (1)$$

$$Ba(NO_3)_2 + 8H_2 \rightarrow 2NH_3 + BaO + 5H_2O \quad (2)$$

$$Ba(NO_3)_2 + 5H_2 \rightarrow N_2 + BaO + 5H_2O \quad (3)$$

$$3Ba(NO_3)_2 + 10NH_3 \rightarrow 8N_2 + 3BaO + 15H_2O \quad (4)$$

The NOx storage capacity (NSC) depends on the population of the Ba phase in the area around the Pt particles. In addition to the reactions on Ba vicinal to Pt, parallel NOx storage reactions (Figure 1) on Ba, uninfluenced by Pt, could also contribute to fast NSC. With a high Ba loading, the region around Pt may be saturated by Ba, and the excess Ba would then be present in the region uninfluenced by Pt. A lower Ba loading may cause under population by Ba in the region around Pt, forming $PtBa/\gamma\text{-}Al_2O_3$ and $Ba/\gamma\text{-}Al_2O_3$ sites, which depend on the Ba loading. Local $Pt/\gamma\text{-}Al_2O_3$ and exposed $\gamma\text{-}Al_2O_3$ would also be available, the population of which would be a function of Pt, Ba loading, and dispersion.

2.2. LNT Catalysts: PGMs, Non-PGM, and Additives

The LNT catalyst essentially contains Pt, Pd, Rh, Ba, Ce, Zr, and some additives. LNT catalysts operate in a cyclic manner, with the gas composition shifting between normally lean and an imposed rich atmosphere; conventionally, the catalyst formulation is $Pt/Ba/Al_2O_3$ (Takahashi *et al*., 1996). The precious metal component is added for the oxidation and reduction reactions, whereas an alkali or alkaline-earth component is added to trap the NOx on the surface as a nitrate. NO_2 is more effectively trapped than NO. Consequently, NO oxidation over the PM sites is a key reaction (Constantinou *et al*., 2013; Chaugule *et al*., 2010).

Pt is a standard LNT component as an active phase but is quite expensive. Recently, some researchers have proposed that Pt-based catalysts can be replaced by perovskite-based catalysts that are used for methane and VOC combustion (Arai *et al*., 1986). A study conducted by Kim *et al*. (2010), included a comparison of different perovskite catalysts for diesel oxidation and with respect to LNT catalyst performance. $La_{0.9}Sr_{0.1}MnO_3$-based catalysts (Kim *et al*., 2010; Constantinou *et al*., 2013), $La_{0.5}Ba_{0.5}CoO_3$ (Onrubia-Calvo *et al*., 2020) and $La_{0.7}Sr_{0.3}CoO_3$ (You *et al*., 2019) have been proposed. Most of the reaction chemistry in the Pt-based catalysts was similar to that of the perovskite-based catalysts. However, the diffusion limitation was stronger on the perovskite, and low-temperature

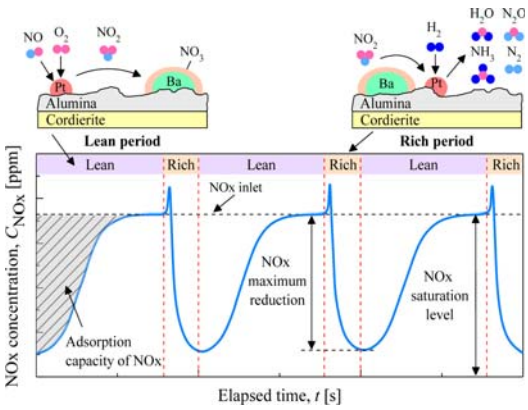

Figure 1. NOx profiles during lean-rich cycles for NOx adsorption and reduction over LNT catalyst.

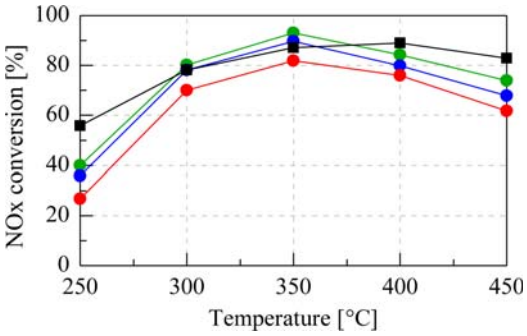

Figure 2. Comparison of NOx conversion over a $La_{0.9}Sr_{0.1}MnO_3$-based LNT (green) with PM loadings of 1.8Pd/0.2Rh (g/L) and commercial LNT (black). Reprinted with permission from Ref. (Kim *et al*., 2010).

regeneration was not a limiting factor for trapping; furthermore, the oxygen storage component consumption was initially inhibited by the presence of nitrates on the surface (Constantinou *et al*., 2013).

Figure 2 shows NOx conversion using a $La_{0.9}Sr_{0.1}MnO_3$-based LNT with PM loadings of 1.8 Pd/0.2 Rh (g/L) (Kim *et al*., 2010). Over 90 % NOx conversion with the $La_{0.9}Sr_{0.1}MnO_3$-based LNT was achieved at 350 °C. The effect of S poisoning and desulfation conditions on the perovskite-based LNT resulted in a loss of approximately 10 % of its initial NOx conversion. After the desulfation process at 700 °C, the NOx conversion was restored to 90 % from 82 % at 350 °C. Under realistic conditions, Sr-doped Co- and Mn-based perovskite catalysts showed NO oxidation activities similar to or higher than those of Pt-based catalysts. The potential use of perovskites for automotive applications is hindered by their susceptibility to deactivation by S. However, the NOx-treating performance of the Pd/perovskite-based diesel oxidation catalyst (DOC) and LNT catalysts demonstrated the potential for Pd/perovskite catalysts as a viable substitute for Pt in diesel after-treatment catalysts.

The metal-based LNT catalyst, $CoOx–K_2CO_3/K_2Ti_8O_{17}$, exhibits an extremely large NSC, a high NOx reduction percentage (99.0 %), and an ultralow NOx to N_2O selectivity (0.3 %). Surface potassium carbonates have been identified as the main storage components, and the single CO_3O_4 oxide acts as active phases for NO oxidation and NOx reduction (Zhang *et al*., 2015).

Several scenarios with additives such as BaO as the main NOx storage material were evaluated. Ceria (CeO_2) possesses a suitable oxygen storage capacity when the engine is operating at stoichiometric conditions. Additionally, Ce promotes H_2 formation under rich conditions via the water-gas shift (WGS) reaction, which can be used for LNT catalyst regeneration and desulfation (Ji *et al*., 2008; Lv *et al*., 2013).

Therefore, Ce-containing LNT catalysts are potential candidates for diesel exhaust after-treatment. The presence

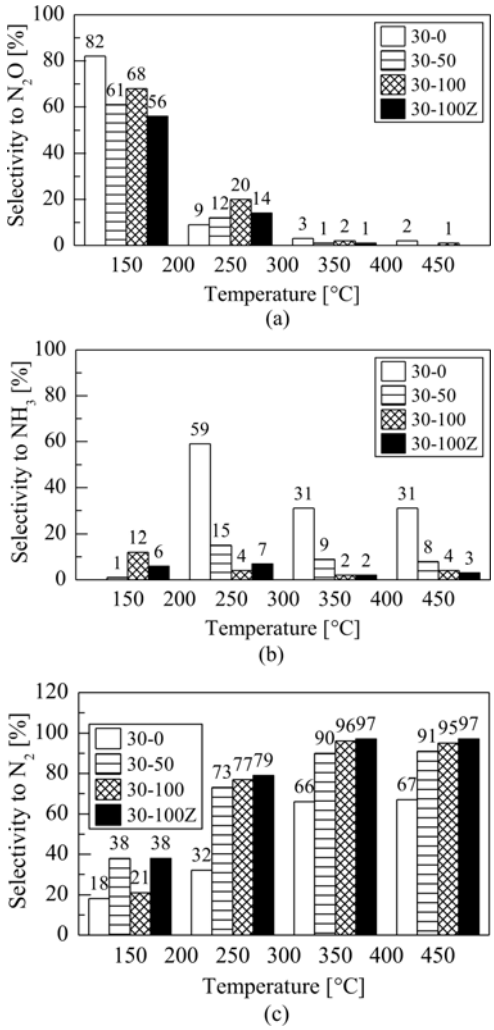

Figure 3. Selectivity to (a) N_2O, (b) NH_3, and (c) N_2 during NOx reduction under NOx storage/reduction cycling. Reprinted with permission from Ref. (Ji *et al*., 2008).

of Ce- increases N_2O selectivity and decreases NH_3. Catalysts containing Ce-Zr exhibit the best de-NOx performance as shown in Figure 3 (Ji *et al*., 2008). This is because of the extremely fast decomposition rate of cerium nitrates under these conditions, as well as the presence of an exotherm from the reaction of the reductants with oxygen stored in the Ce phase, and/or localized reductant shortages at the reaction front owing to the consumption of the reductant by stored oxygen. Pt-BaO-CeO_2 and Cu-CeO_2 deposited on the reduced Al_2O_3 (PBCrA + CCrA) demonstrate superior low-temperature activity and hydrothermal stability, whereas the absence of Al_2O_3 or the use of intact Al_2O_3 support severely degrades the LNT performance after hydrothermal aging at 750 °C for 25 h using 10 % H_2O/air as shown in Figure 4 (Kim *et al*., 2020). The high Ba dispersion on CeO_2 is an advantage for Ba–Ce contact and NOx trapping. Moreover, the Ba sites in close contact with oxygen from CeO_2 can be effectively

used to form nitrates at low temperatures, causing higher stability than the Ce nitrates (Lv *et al*., 2013).

Numerous studies have focused on the reactivity of Ba-containing catalysts; however, few studies on the specific storage characteristics of K-based catalysts have been reported (Toops *et al*., 2005; Castoldi *et al*., 2010; Kim *et al*., 2012a). These works focus on the analysis of the reduction steps when K replaces Ba as the storage component. In the K-based catalyst, Pt plays a significant role in the oxidation of the surface nitrites to nitrates and contributes to the destabilization of the K–CO_2 bonds, allowing additional nitrate formation. However, when CO_2 is included in a feed stream with NO and O_2, the amount of K-based nitrate storage decreases (Toops *et al*., 2005).

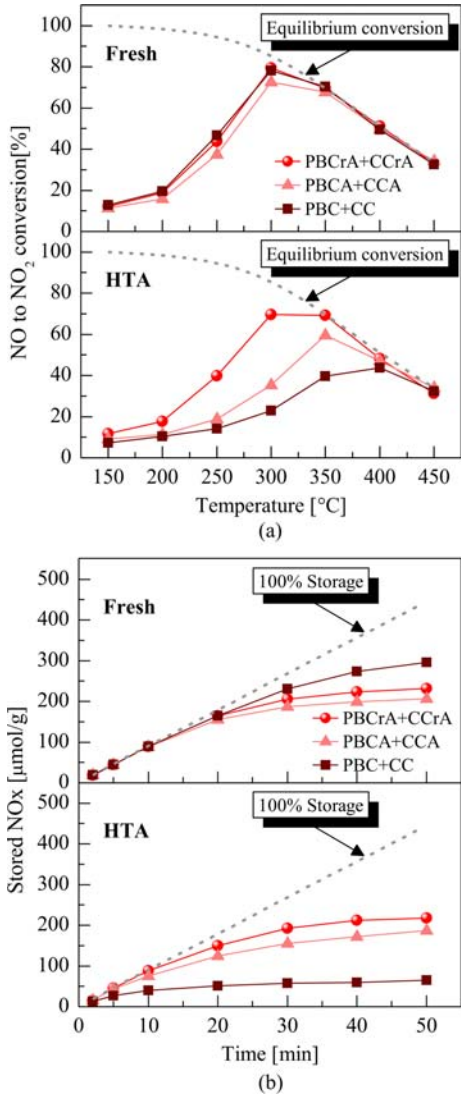

Figure 4. (a) The conversion of NO to NO_2, showing NO oxidation capacity (NOC) and (b) the amount of stored NOx over time at 200 °C under a lean condition, showing NOx storage capacity (NSC). Reprinted with permission from Ref. (Kim *et al*., 2020).

Figure 5 shows the N_2 selectivity with the PtK/Al_2O_3 and PtBa/Al_2O_3 catalysts. During the regeneration process, the N_2 selectivity of PtK/Al_2O_3 catalyst is higher than that of the PtBa/Al_2O_3 catalyst. This is because, in the former case, the onset of the H_2^+ nitrate reaction forming NH_3 occurs at temperatures very close to the threshold for the NH^{3+} nitrate reaction to form N_2. NH_3 readily reacts with the surface nitrates to form N_2 (Castoldi *et al*., 2010). The LNT forms more thermally stable nitrate species with the increase of the K loading from 5 wt% to 10 wt%. Limitations such as sulfur poisoning/removal affecting the durability of the LNT are yet to be overcome for this new class of catalysts because they are being considered for application in high temperature LNT materials (Kim *et al*., 2012a).

In commercial applications, Pt and Rh are mainly used as precious metal catalysts. Recently, Pd has also been adopted to enhance high temperature reactions with Pt and Rh. For NOx adsorption, as explained above, Ba is the main material, whereas K and Na are being carefully considered in multiple studies including Mg, Sr, and Ca. Because diesel fuel has a sulfur component, its oxidation forms in the exhaust gases cause the chemical poisoning of the NOx adsorbing materials.

Although sulfur poisoning is a reversible chemical reaction, it deteriorates adsorption capacities when it is built-up over long operation times. To resolve the issue of sulfur poisoning and decrease the desulfurizing

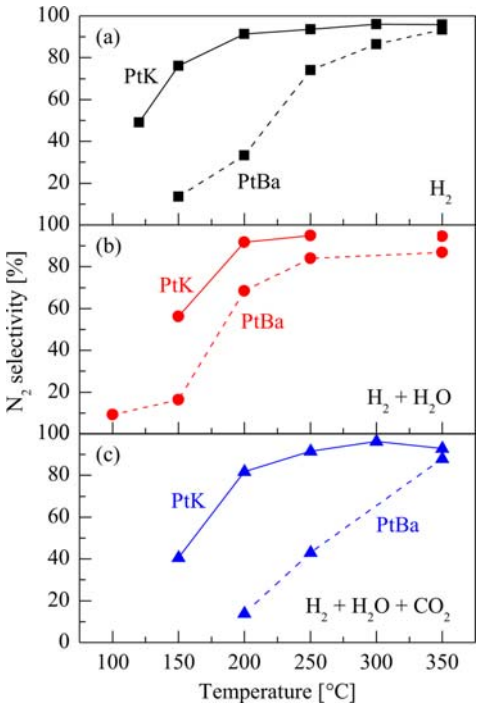

Figure 5. N_2 selectivity for PtK/Al_2O_3 and PtBa/Al_2O_3 catalysts; (a) H_2, (b) H_2 + H_2O, and (c) H_2 + H_2O + CO_2. Reprinted with permission from Ref. (Castoldi *et al*., 2010).

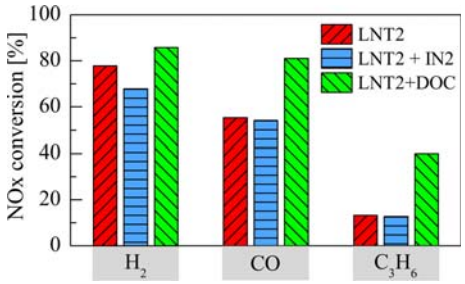

Figure 6. NOx conversions over a single steady-state lean/rich cycle-comparison of the 2-layers catalysts using different reductants at 250 ℃. Reprinted with permission from Ref. (Vaclavik *et al*., 2016).

temperature, which can reduce fuel penalty during NSC regeneration, Ce and Zr are recently being used as additive catalysts.

Recent efforts in emission control catalyst aim to save space and cost by combining different catalytic functions in a single multi-layered monolith reactor (Morita *et al*., 2007; Vaclavik *et al*., 2016). However, the overall efficiency of the converter, and particularly the bottom layer performance, can be negatively affected by transport limitations. In the LNT + DOC two-layer catalyst, the DOC layer on top of the LNT improves the catalytic performance at lower temperatures by increasing the effective NSC (because of NO oxidation activity) and enhances regeneration efficiency because of the WGS, steam reforming, and NH_3 re-oxidation, as shown in Figure 6 (Vaclavik *et al*., 2016). Figure 6 shows that the first coat is the LNT layer, which is subsequently overlaid with an inert γ-Al_2O_3 layer. Morita *et al*. (2007) developed a two-layer lean NOx catalyst for diesel engines, comprising a Ce-rich LNT catalyst bottom layer and an SCR-type catalyst top layer (Morita *et al*., 2007). The bottom layer acts as the NOx storage catalyst under lean conditions; under rich conditions, the stored NOx is reduced to NH_3, which is then stored in the top layer where it is available for reaction with NOx under lean conditions.

2.3. Improvement of De-NOx Performance

Initially, deactivation during the rich phase is omitted by the O adsorbed species. However, the formation of amorphous carbon, and the significant deactivation of noble-metal sites occur in the presence of C_2H_2. The significant impact of C_2H_2 activation in reforming the reaction during deactivation is further confirmed at lower temperatures compared to the C_2H_4 and C_3H_6 HC alkenes with weaker adsorption (Simböck *et al*., 2019).

Park *et al*. (2011, 2012) reported a combined system of a DME steam reforming (SR) catalyst and the LNT to improve de-NOx performance. In the system, the DME SR catalyst (Cu/ZSM-5 based) produced H_2 and CO, which were used as reductants for the LNT catalyst. The de-NOx performance of the combined system was improved by 20

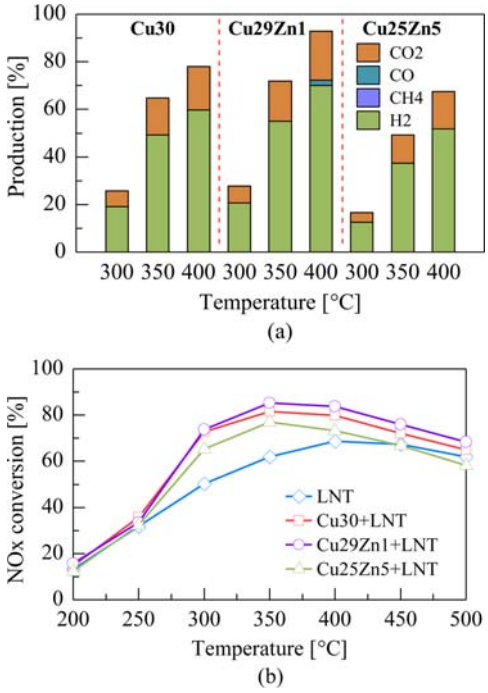

Figure 7. (a) H_2 production by SR catalysts and (b) NOx conversion of the combined system of SR + LNT catalysts. Reprinted with permission from Ref. (Park *et al.*, 2011).

% compared to the LNT alone (Figure 7) (Park *et al.*, 2011).

In the 1980s, researchers developed a three-way catalyst (TWC) for a gasoline vehicle. They evaluated the control of the air-fuel ratio of the engine to be close to the stoichiometric air-fuel ratio to maximize the purification efficiency of the TWC. Similarly, a method for injecting HCs in rapid pulses (frequency, amplitude, and duty cycle) was considered to improve the de-NOx performance of the LNT (Reihani *et al*., 2018). The optimal pulsing frequency for the NOx conversion was in the order of 0.5 ~ 1 Hz (Figure 8). Furthermore, controlling the spray behavior of the reductant is important in rich conditions (Park *et al*., 2018).

Figure 9 shows the NOx conversion as a function of the delivered reductant per pulse for different pulsing frequencies. Because the duty cycle of the pulses was constant, the average reductant flow and consequently the fuel penalty, were constant for points with the same rich pulse amplitude (λ_{pulse}); these are shown as dotted isofuel penalty curves. The maximum NOx conversion as a function of the pulsing frequency was obtained at a λ_{pulse} of 0.8 ~ 0.73. The NOx conversion improved as the pulses became richer at a given pulsing frequency. However, when the pulses became richer than λ_{pulse} = 0.8 to 0.75, the slope of the isofrequency curves decreased (e.g. compare the slope at points A and B). Regardless of the pulsing frequency, the NOx conversion was very low at 600 ℃

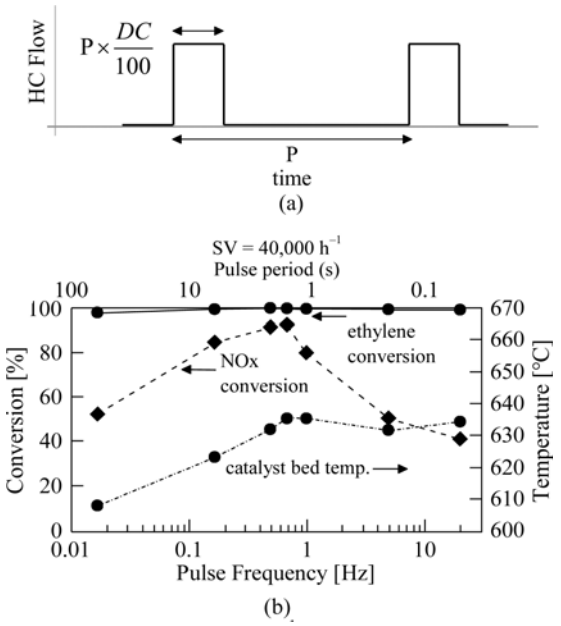

Figure 8. (a) Definition of total rich/lean cycle period (P (s)) and duty cycle (DC (%)), and (b) reductants frequency sweep results at 600 °C inlet temperature (15 % DC, λ_{pulse} = 0.83). Reprinted with permission from Ref. (Reihani *et al*., 2018).

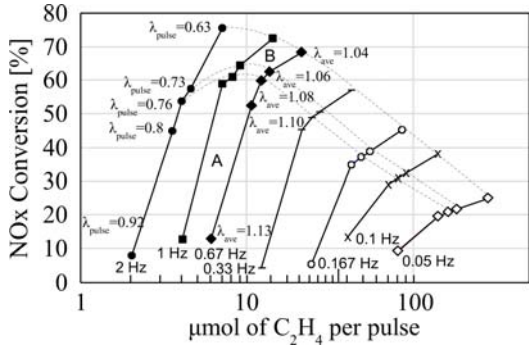

Figure 9. The effect of pulse magnitude and pulsing frequency on NOx conversion, plotted as a function of moles of ethylene/pulse for 15 % pulse DC, inlet T = 600 °C, and SV = 30,000 h^{-1}. Reprinted with permission from Ref. (Reihani *et al*., 2018).

with lean or stoichiometric pulses. Although the time-averaged flow remained net lean, rich pulses were required to achieve a significant NOx conversion.

2.4. Durability: Sulfur Poisoning and Thermal Aging

In most countries around the world, regulations on sulfur content in diesel fuel are maintained below 10 ppm. However, sulfur poisoning is a major cause for performance degradation and hinders the broad market penetration of LNT systems. As shown in Figure 10, significant NOx and NO breakthroughs occurred as the

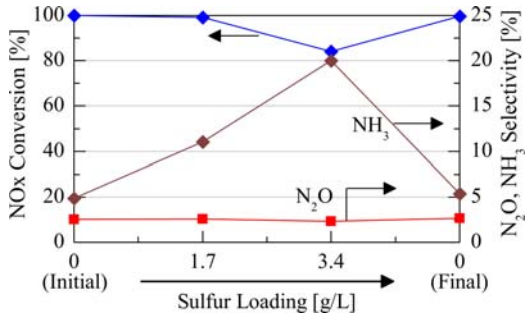

Figure 10. NOx conversion and N_2O and NH_3 selectivities as a function of catalyst sulfur loading. Reprinted with permission from Ref. (Choi *et al*., 2007).

sulfur dosing increases, lowering the NOx conversion to 84 %. The subsequent desulfation fully recovered the NOx conversion. The N_2O selectivity remained low (2 ~ 3 %) with slight dependence on the sulfur loading. The NH_3 selectivity increased significantly with increasing sulfur loading (Choi *et al*., 2007; Choi *et al*., 2008).

Sulfur resistance catalysts were evaluated to solve the sulfur poisoning problem (Kwak *et al*., 2008). Figure 11 shows the NOx conversion changes by sulfation and de-sulfation treatment for the ceria- and alumina-based catalysts. After the SO_2 treatment, the NOx conversion of the alumina-based catalyst was reduced from 48 % to 23 %, whereas it decreased from 60 % to 43 % with the Ce-based catalyst. After SO_2 exposure, the NOx conversion on the alumina-based catalyst completely disappeared at the start time. Conversely, the Ce-based catalyst showed only a small change. Presumably, the sulfur-poisoning mechanism on $Pt/BaO/Al_2O_3$ catalysts is initiated by the oxidation of SO_2 on the metallic Pt particles, followed by a spillover of the produced SO_3 to the vicinal barium phase to form barium sulfate near the Pt clusters (Matsumoto *et al*., 2000). The Ce-based catalyst, and active BaO phase near the Pt clusters remained available for NOx storage even after SO_2 exposure. The sulfur resistance of the ceria-based catalyst was remarkable (Kwak *et al*., 2008).

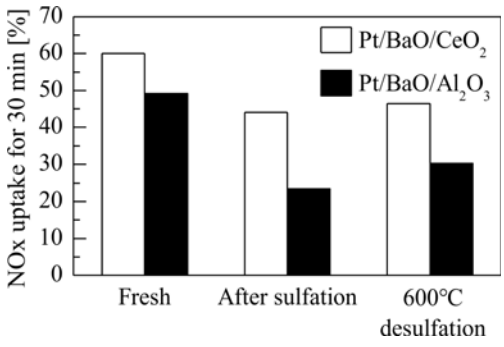

Figure 11. NOx conversion by sulfation and de-sulfation for $Pt/BaO/CeO_2$ and $Pt/BaO/Al_2O_3$. Reprinted with permission from Ref. (Kwak *et al*., 2008).

A conceptual model of lean and rich sulfation dynamics on the catalysts was proposed (Ottinger *et al*., 2012). SO_2 is efficiently stored in a spillover mechanism near the Pt particles, such that the population of SO_2 on the Pt is low. As the surrounding oxides become sulfated, the transfer of SO_2 from the Pt to the oxide slows, and the population increases on the Pt surface. The ceria–zirconia phase contains O_2 that is available to form sulfates under rich conditions. Therefore, when the conditions are switched from lean to rich, the Pt-bound SO_2 is captured in the ceria–zirconia phase. The most striking effect of employing a ceria–zirconia support with Ba occurs in the desulfation profiles. The O_2 storage behavior of ceria–zirconia plays a role in the storage of sulfur during cycling conditions (Ottinger *et al*., 2012). The adsorbed sulfur can then be desorbed via the following reactions:

$$BaSO_4 + H_2 \rightarrow BaO + SO_2 + H_2O \quad (5)$$

$$BaSO_4 + 4H_2 \rightarrow BaO + H_2S + 3H_2O \quad (6)$$

Hydrogen reacts instantly with the oxygen adsorbed on the catalyst surface, and the NOx stored in the catalyst. However, it may be difficult to promote sulfur desorption using the hydrogen in the exhaust. Matsumoto *et al*. (2000) designed a catalyst that would enhance sulfur desorption by forming hydrogen on the catalyst, particularly in the vicinity of the NOx storage element (Figure 12). Rh/ZrO_2 is an advantageous catalyst for the formation of H_2 under rich operating conditions.

The sintering of PGMs on the catalyst is because of high temperature exposure. When the LNT is exposed to high temperatures in the rich spike period, it is faced with two issues with respect to thermal aging: the precious metal catalyst sintering, and the aging of Ba and additives. Additionally, the modification of Ti has a significant impact on thermal durability. The Al_2O_3-TiO_2 nanofibrous catalyst improves thermal durability and S resistance relative to γ-Al_2O_3 because of the Ti or Ba/Ti interactions. Incorporating Ti in the nanofibrous Al structure was found to also promote sulfur desorption (Pieta *et al*., 2011).

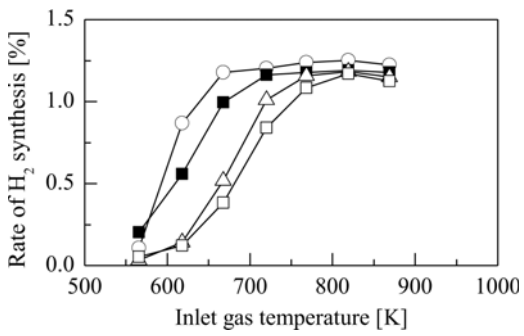

Figure 12. Formation of H_2 on catalyst under a flow of rich gas. Catalyst: Rh/ZrO_2 (circle), Rh/Al_2O_3 (closed square), Pt/ZrO_2 (triangle), and Rh/TiO_2 (square). Reprinted with permission from Ref. (Matsumoto *et al*., 2000).

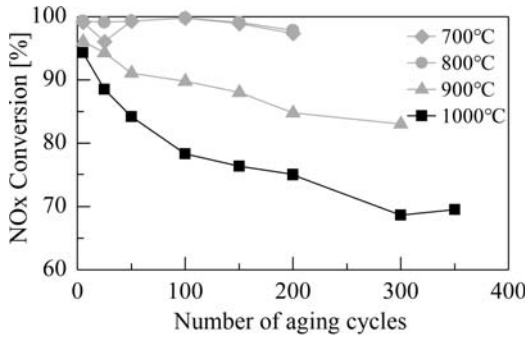

Figure 13. NOx conversion at 300 °C after aging at the indicated nominal aging temperatures. Reprinted with permission from Ref. (Ottinger *et al*., 2011).

Figure 13 shows that NOx conversions at 300 °C are maintained when aging at 700 and 800 °C, but there is a significant decrease when the samples are heated to 900 and 1000 °C (Toops *et al*., 2007; Ottinger *et al*., 2011). The following deactivation mechanisms are accelerated at LNT catalyst temperatures exceeding 800 °C: (i) loss of dispersion of the PM, (ii) phase transitions of the adsorbent material and support, and (iii) loss of the total surface area (Toops *et al*., 2007). The BET surface area at 700 and 800 °C results in a maximum surface area loss of only 18 %, whereas aging at 900 and 1000 °C results in a much higher (44 %) reduction. The average PM size increases from 2.5 nm in fresh LNT to 26 nm in LNT aged at 1070 °C. Reductions in the PM dispersion resulting from aging cause a significant increase in the NO turnover frequency at 400 °C. The availability and stability of the NOx storage site reduced after aging at 930 and 1070 °C, respectively, are linked to the loss of the Al_2O_3 storage sites as well as the re-dispersion of Ba into a phase with a lower NOx capacity (Ottinger *et al*., 2011). Given the importance of the Pt–Ba interface, it follows that high Pt loadings on the BaO/Al_2O_3 component are beneficial for catalyst performance because they ensure a high degree of Pt–Ba contact. The higher Rh loaded catalyst showed slightly better low-temperature NOx reduction activity (Ji *et al*., 2011).

2.5. Application of De-NOx Techniques: LNT+SCR and LNT+SDPF

A dual-bed catalytic converter consisting of the LNT + SCR or SCR + LNT catalysts is typically employed for high-concentration NOx removal under the lean-burn condition. Seo *et al*. reported a combined LNT + SCR catalyst system (Snow *et al*., 2007; Seo *et al*., 2011). When H_2 is supplied as the reductant, NH_3 is generated as an intermediate product during the reduction reaction of the nitrate $(NO_3)_2$ stored in the Ba site on the LNT catalyst (Seo *et al*., 2011; Wang *et al*., 2011). NH_3 is formed because of the reduction of the adsorbed NOx species in stoichiometric conditions. The NH_3 formed by the LNT is

then utilized by the downstream SCR catalyst to reduce NOx in the exhaust gas. Figure 14 shows the NOx conversion of the LNT catalyst, and the combined LNT + SCR system. Regarding the fresh catalyst, the NOx conversion of the combined system was approximately 15 % higher than that of the LNT catalyst at the low-temperature area. The formed NH_3 emitted from the LNT catalyst should serve as a reactant for the downstream SCR catalyst (b). The NOx conversion of the combined system (aged at 750 ℃) was 10 ~ 30 % higher than that of the LNT catalyst. The N_2O slip of the aged catalysts was small (c).

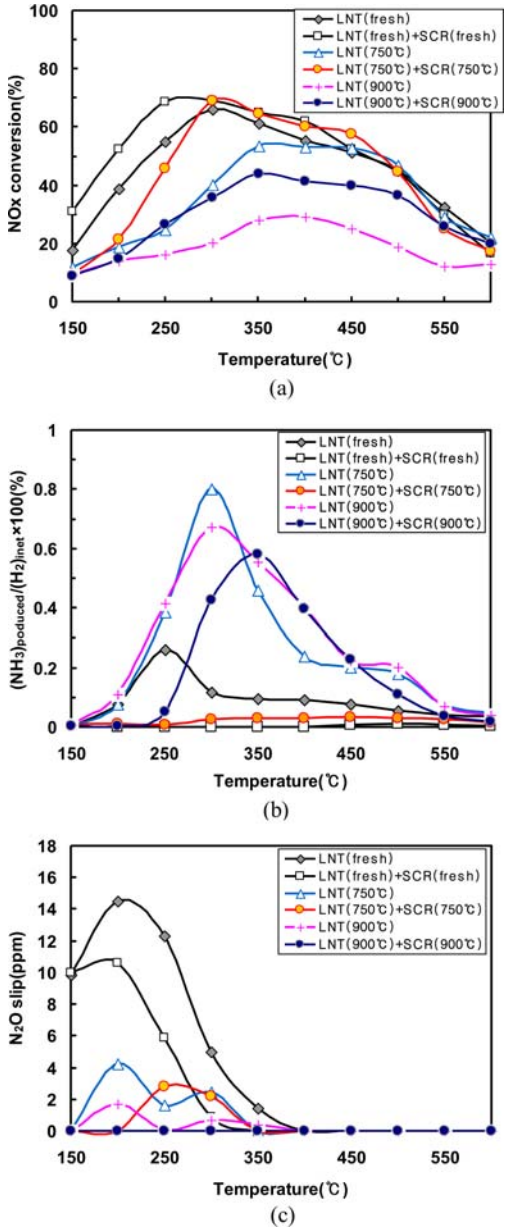

Figure 14. NOx conversions and NH_3 and N_2O production of the combined system of LNT + SCR; (a) NOx conversion, (b) NH_3 ratio, and (c) N_2O slip. Reprinted with permission from Ref. (Seo *et al*., 2011).

The combined system compensates for the de-NOx performance, and reduces the NH_3 and N_2O slip, although the catalysts are aged hydrothermally (Seo *et al*., 2011).

The lean NOx could be partially reduced over the upstream SCR catalyst (Cu/Al_2O_3) by C_3H_6 in the stream, significantly increasing the efficiencies of both the NOx storage and reduction over the downstream LNT catalyst ($La_{0.7}Sr_{0.3}CoO_3$) (You *et al*., 2019). The combined LNT + SCR or SCR + LNT after-treatment techniques compensate for the defects of the individual techniques and have great application potential in the lean de-NOx technique (Kang *et al*., 2018). Recently, LNT and SCR catalysts have been applied on the diesel particulate filter (DPF) to simultaneously remove NOx and PM. Choi and Lee proposed the technology of LNT/DPF for the simultaneous removal of NOx and PM from diesel vehicles (Choi and Lee, 2014). The NOx conversion of the LNT(2Pt20Ba5Co)/DPF improved to 55 % at 310 ℃ when 5 wt% cobalt was added to the $2Pt20Ba/Al_2O_3$ catalyst to improve the NOx conversion of the LNT/DPF. Kang *et al*. (2018) reported a hybrid system of the LNT/DPF + SCR/DPF catalyst. The de-NOx and de-PM of the hybrid system were superior to those of the single LNT/DPF system. This is because NO_2 and NH_3 that form LNT/ DPF under a rich air-to-fuel ratio are used as a reductant for the SCR/DPF catalyst of the hybrid system of LNT/DPF + SCR/DPF. Additionally, the SCR/DPF increases the NOx conversion through HC-SCR.

3. SCR OF NOx BY UREA/NH_3

3.1. NH_3-SCR Process

Urea-SCR technology is the most widely used technology for NOx reduction owing to its impressive de-NOx performance and wide operating temperature. The urea-SCR system uses ammonia (NH_3) as the primary reductant, which is derived from an aqueous solution of urea. This is because it is difficult to deal with gaseous NH_3 in terms of storage, toxicity, and safety. Recently, to comply with emission standards, the urea-SCR system has been employed in non-road diesel engines (Han *et al*., 2019). The typical configuration of urea-SCR installed in diesel vehicles is shown in Figure 15.

Aqueous urea is injected and uniformly atomized via the

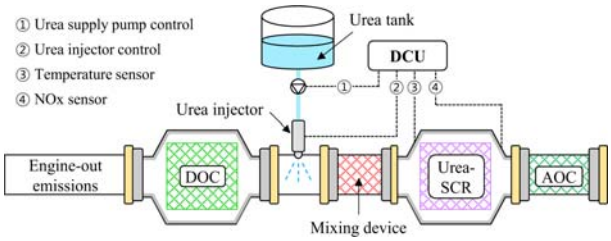

Figure 15. Layout of automotive urea-SCR system equipped with DOC and AOC.

exhaust gas stream; the pure urea then undergoes several reactions (reactions (7) ~ (10)) to yield gaseous NH_3 as an available reductant: Reaction (7) involves the evaporation of atomized urea from the aqueous solution to molten urea. It is then thermally decomposed in reaction (8), yielding one mole of NH_3 and isocyanic acid (HNCO). Subsequently, HNCO reacts with H_2O via the hydrolysis of HNCO (reaction (9)) to yield more NH_3 (Koebel *et al*., 2000). The overall steps are summarized in reaction (10), where one mole of urea is converted to two moles of gaseous NH_3.

$$NH_2\text{-}CO\text{-}NH_2 \rightarrow NH_2\text{-}CO\text{-}NH_2(\text{molten}) + xH_2O \quad (7)$$

$$NH_2\text{-}CO\text{-}NH_2(\text{molten}) \rightarrow NH_3(g) + NHCO\ (g) \quad (8)$$

$$NHCO\ (g) + H_2O\ (g) \rightarrow NH_3(g) + CO_2\ (g) \quad (9)$$

$$NH_2\text{-}CO\text{-}NH_2(aq) + H_2O\ (g) \rightarrow 2NH_3(g) + CO_2\ (g) \quad (10)$$

Basically, the reduction of NOx to N_2 by the urea-SCR process occurs in three steps, including standard, fast, and slow reactions; the molar ratios of NO, NO_2, and NH_3 are the distinctive factors that determine the dominant reaction routes:

$$4NH_3 + 4NO + O_2 \rightarrow 4N_2 + 6H_2O \quad (11)$$

$$2NH_3 + NO + NO_2 \rightarrow 2N_2 + 3H_2O \quad (12)$$

$$4NH_3 + 3NO_2 \rightarrow 3.5N_2 + 6H_2O \quad (13)$$

Reaction (11), where the reduction of NO to N_2 occurs, is termed as the standard SCR reaction. This is the primary reaction because the major constituents of NOx (engine-out emissions) are NO and NO_2 in proportions of approximately 90 % and 10 %, respectively (Mohan *et al*., 2020); this reaction is very slow without oxygen, and is not applicable for exhaust after-treatment systems. Owing to the presence of DOC upstream of the SCR catalyst, the oxidation of NO to NO_2 occurs under a lean-exhaust atmosphere, which causes the fastest reaction shown in reaction (12); this reaction with equimolar NO and NO_2 is the fastest and highly suitable to reduce NOx with NH_3. However, if the NO_2 is predominant in the exhaust, reaction (13), which is the slowest reaction, is predominant in the SCR reaction (Jung *et al*., 2017).

3.2. NH_3-SCR Catalysts

Catalytic materials are significant factors for the NH_3-SCR process because their de-NOx performance is highly dependent on the type of active metals, which are uniformly distributed on the catalytic supports. Additionally, the preparation methods affect the catalytic activity; the major techniques for the catalytic preparation are aqueous ion exchange (Peng *et al*., 2020), solid-state ion exchange (Urrutxua *et al*., 2019), impregnation (Cha *et al*., 2016), mechanical mixing (Pan *et al*., 2020), and co-precipitation (Xiong *et al*., 2020). Among the various synthetic methods, the metal ion-exchange method with zeolites is widely used because the cationic metals can be exchanged with the anionic zeolite sites, which act as active sites for NOx reduction. Although many studies have focused on the preparation methods for improving de-NOx performance, the best preparation method is still under debate because of varying mass transportation, different adsorption characteristics of reactants, and physicochemical properties.

3.3. Catalytic Activity of NH_3-SCR Catalysts

Over the last few decades, copper (Cu) and iron (Fe) exchanged zeolites (such as SSZ-13, ZSM-5, and BETA) have become popular for their comparable de-NOx performance and relatively lower costs compared to TiO_2 (Cheng and Bi, 2014). These catalysts have demonstrated excellent NH_3-SCR activity. The most studied catalysts are Cu and Fe ion-exchanged ZSM-5 (Cu/ZSM-5 and Fe/ZSM-5), owing to their high resistance to thermal stability and sulfur poisoning. The primary difference between Cu/ZSM-5 and Fe/ZSM-5 is the active operating temperature for NOx abatement.

As illustrated in Figure 16, Cu/ZSM-5 is preferred below reaction temperatures of 350 °C, whereas Fe/ ZSM-5 is more active than Cu/ZSM-5 and V_2O_5/WO_3-TiO_2 at high temperatures above 500 °C (Kröcher, 2007). To widen the NOx reduction operating temperature window, a combination of Cu and Fe is employed as the active phase; the reaction tests of the catalysts indicate minor positive effects of Fe addition in Cu + Fe/BEA where NH_3 activity, N_2 selectivity, and hydrothermal stability are slightly improved (Wang *et al*., 2019a).

According to the reports in the literature, the catalytic deactivation phenomenon may have numerous origins such as thermal, mechanical, and chemical deactivation (Peng *et al*., 2014; Auvray *et al*., 2019; Liu *et al*., 2020). Hydrothermal stability is significant for the practical application of the NH_3-SCR system because the thermal energy induces wash coat sintering, resulting in the severe

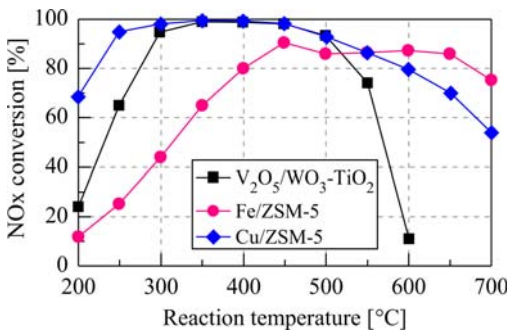

Figure 16. De-NOx performance at a function of reaction temperature over V_2O_5/WO_3-TiO_2, Fe/ZSM-5, and Cu/ZSM-5. Feed conditions: 1000 ppm NO, 10 % O_2, 5 % H_2O, 1000 ppm NH_3 at GHSV = 52,000 h^{-1}. Reprinted with permission from Ref. (Kröcher, 2007).

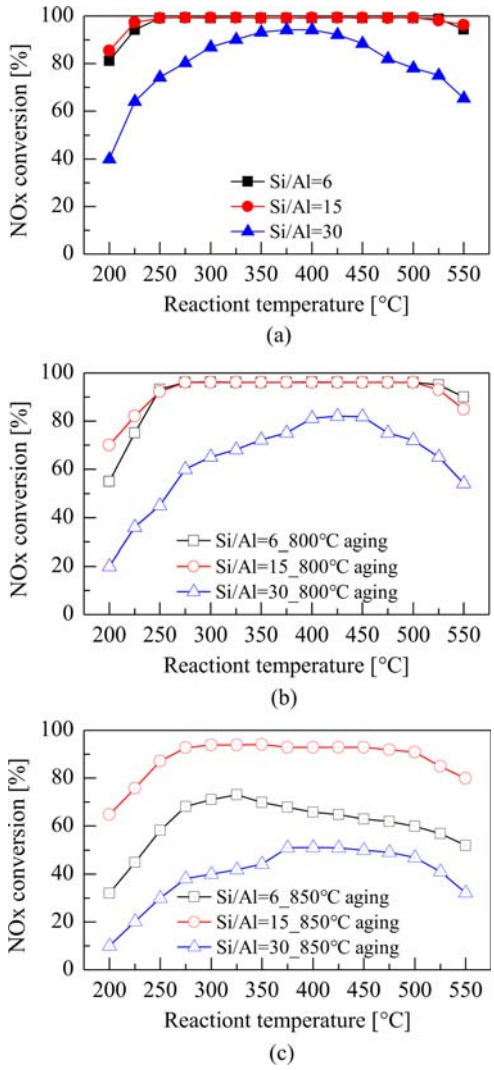

Figure 17. NH_3-SCR performance of the fresh and hydrothermally aged catalysts over Cu/SSZ-13 according to Si/Al ratios; (a) fresh, (b) 800 ℃ aging, and (c) 850 aging. Feed conditions: 1,000 ppm NO, 1,100 ppm NH_3, 5 % O_2, 10 % H_2O with balance N_2 at GHSV = 30,000 h^{-1}. Reprinted with permission from Ref. (Fan *et al*., 2018).

deactivation of the SCR catalysts. Hydrothermal aging causes the dealumination of the zeolite frameworks and agglomeration of the active Cu sites for NOx reduction (Song *et al*., 2017; Zhao *et al*., 2019a). To suppress the dealumination of zeolites, there have been substantial studies focusing on the compositional Si/Al ratio (Wang *et al*., 2014), pore distribution (Zhang *et al*., 2016), zeolite size (Peng *et al*., 2018), etc. Hydrothermally aged Cu/SSZ-13 catalysts have been studied recently, and there have been meaningful results in practical terms (Zhao *et al*., 2019b; Shan *et al*., 2020). Figure 17 shows a comparison of the catalytic performance of NOx reduction over fresh and hydrothermally aged Cu/SSZ-13 with different Si/Al ratios

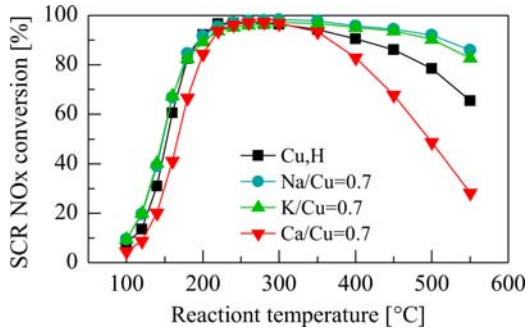

Figure 18. NOx conversion for standard SCR on hydrothermally aged Cu-additive/SSZ-13 catalysts at additive/Cu = 0.7. Feed condition: 360 ppm NO, 360 ppm NH_3, 2.5 % H_2O, 14 % O_2 at GHSV = 100,000 h^{-1}. Reprinted with permission from Ref. (Cui *et al*., 2019).

of SSZ-13 zeolite. Si/Al ratios of 6 and 15 catalysts exhibited over 95 % NO conversion from 225 to 550 ℃, respectively. Conversely, the Si/Al ratio of 30 catalysts showed an inferior NOx conversion at all reaction temperatures. The catalytic performance was maintained after hydrothermal aging at 800 ℃ for 12 h with minor decreases at low temperatures (≤ 250 ℃). Further hydrothermal aging at 850 ℃ induced a severe catalytic deactivation over Si/Al ratios of 15 and 30, whereas a Si/Al ratio of 15 maintained most of the NOx conversion after the same aging treatment.

Metallic additives including alkali or alkaline-earth metals (Na, K, and Ca) (Cui *et al*., 2019), Zn (Xu *et al*., 2020), and MnOx–CeO_2 (Liu *et al*., 2017a) are employed to further enhance the catalytic stability of Cu/SSZ-13. After hydrothermally aging, CuNa/SSZ-13 and CuK/SSZ-13 exhibit high hydrothermal stability within a wide temperature window of 200 ~ 550 ℃ compared to Cu/SSZ-13, as illustrated in Figure 18. Notably, this hydrothermal stability is among the highest reported in literature on Cu/SSZ-13 catalysts hydrothermally aged at 800 ℃ (Cui *et al*., 2019). In contrast, the hydrothermal stability of CuCa/SSZ-13 is substantially inferior at low and high temperatures.

Considering the emission conditions of actual vehicles,

Table 1. Hydrocarbon-poisoning species of various catalysts reported in literature.

Catalyst	HC species	Reference
Cu/SSZ-13	Propene (C_3H_6)	Zhang *et al*., 2019a
Cu/ZSM-5	Ethene (C_2H_4)	Shibata *et al*., 2019
Fe/ZSM-5	Propene (C_3H_6)	Zhang *et al*., 2018
Cu/BEA	Propane (C_3H_8)	Zhao *et al*., 2017
Ce/BEA	Propene (C_3H_6)	Shi *et al*., 2017

engine-out exhausts always contain a variety of unburned HCs (UHCs) ranging from light to heavy HCs. Numerous studies have focused on the effect of the poisoning of HC species on various types of catalysts, as summarized in Table 1. Coexistent HCs induce a negative effect on catalytic activities in the NH_3-SCR process. Generally, HC species inhibit the catalytic reaction of NOx reduction via different mechanisms or pathways such as i) competitive adsorption with NH_3 (or NO) and direct adsorption on the catalytic surface (Ma *et al*., 2015), ii) blocking of active sites owing to coke deposition (Feng *et al*., 2016), iii) inhibition of the required reaction intermediates (Luo *et al*., 2012). Recently, these issues have been mitigated by small-pore (8-membered ring) frameworks. Cu/SSZ-13 catalysts have been found to exhibit a superior resistance to HC poisoning compared to Cu/ZSM-5 and Cu/BEA (Deka *et al*., 2013). SSZ-13 adopts the chabazite (CHA) structure, which is constructed by stacking double-six-membered rings in an AABBCCAA sequence. This allows for the formation of large CHA cavities, accessible through a three-dimensional eight-membered pore-opening system (Gao and Szanyi, 2018). Catalytic deactivation by HC poisoning still needs to be resolved for automotive applications.

As explained above, zeolites with an optimized Si and Al ratio to control pore size and enhance selective reaction are the key component in the light duty application of SCR. Cu and Fe exchanged zeolites are used in commercial applications to improve selective reaction and increase NH_3 adsorption. Normally, Fe-SCR demonstrates better performance at high temperatures, whereas Cu-SCR performs better at lower temperatures. Because cordierite material is mainly used as a substrate, the major components of the SCR wash coat are alumina with TiO_2 support to ensure adhesion for long durability.

4. SCR OF NOx BY HC

4.1. HC-SCR Process

The major drawback of the urea/NH_3-SCR system is that it requires additional space for storage, deposition of the aqueous urea solution, and complicated injection equipment for supplying the reductant. Therefore, HCs have been considered as an alternative reductant for the de-NOx process. In the 1990s, a pioneering study was conducted with HCs as the reductants during the de-NOx process (Held *et al*., 1990; Iwamoto *et al*., 1990; Iwamoto *et al*., 1991). Thereafter, the SCR of NOx by HCs (HC-SCR) emerged as a potential de-NOx technology for NOx reduction in excess-oxygen environments. The additional advantages of directly using on-board fuels without the need for additional space to store the reductant makes this system more attractive (Lee *et al*., 2020). The primary features of the reaction pathways for the HC-SCR process are divided into the following three categories:

i) Oxidation of NO to NO_2 and selective reaction with HCs (Descorme *et al*., 1996; Miller *et al*., 1998; Yan *et al*., 1998)

$$NO + 1/2O_2 \rightarrow NO_2 \quad (14)$$

$$NO_2 + HC \rightarrow N_2 + CO_2 + H_2O \quad (15)$$

ii) Reaction of activated HCs with NOx (Smits and Iwasawa, 1995; Sun *et al*., 1997)

$$HC + O_2 \rightarrow HC^* + CO_2 + H_2O \quad (16)$$

$$NOx + HC^* \rightarrow N_2 + CO_2 + H_2O \quad (17)$$

iii) NO decomposition and regeneration of active sites by HCs (Burch *et al*., 1994; Burch and Watling, 1997)

$$2NO \rightarrow N_2 + 2O\ (ads) \quad (18)$$

$$NOx + HC^* \rightarrow N_2 + CO_2 + H_2O \quad (19)$$

The HC-SCR process is initiated by the oxidation of NO to NO_2 as an indispensable reaction, followed by the reduction of NO_2 with the HC into N_2. The second reaction pathway is related to the reaction intermediates by the partially oxidized HCs (HC*) with the coexistent O_2, which reacts with NOx to forminto N_2, CO_2, and H_2O. The third reaction pathway is the catalytic decomposition of NO to N_2, where the adsorbed O_2 on the catalyst surface reacts with HC to form CO_2 and H_2O.

4.2. Improvement of De-NOx Performance

Since the discovery of the feasibility of HC-SCR for catalytic NOx abatement, a variety of catalytic materials have been studied as active phases for improving de-NOx performance. One of the limitations of HC-SCR is its low catalytic performance and narrow temperature windows for NOx reduction, owing to the poor selectivity of HCs toward NOx (Cheng and Bi, 2014). To improve the de-NOx performance and extend the active temperature windows, catalysts with transition metals supported on zeolites (MOR, SSZ-13, ZSM-5, and BEA) and PGMs (e.g. Au, Pd, and Pt) supported on metal oxides have been employed for the HC-SCR process, as summarized in Table 2.

Lee *et al*. (2019a) evaluated the effect of zeolite topology (SSZ-13, ZSM-5, and BEA zeolite) and Cu content (Cu 1 ~ 10 wt%) on the C_4H_{10}-SCR process. 2Cu/ZSM-5 exhibited the best de-NOx performance with approximately 74 %, followed by 10Cu/BEA (58 %), and 1Cu/SSZ-13 (38 %), as illustrated in Figure 19 (Lee *et al*., 2019a). These results were related to the geometry-limited diffusion of the reducing agent to the active sites in the ZSM-5 and BEA zeolite channels; however, they were considerably restricted in the SSZ-13 zeolite (Lee *et al*., 2019a). The catalytic activities of Cu/zeolite catalysts are known to be sensitive to hydrothermal aging. As illustrated

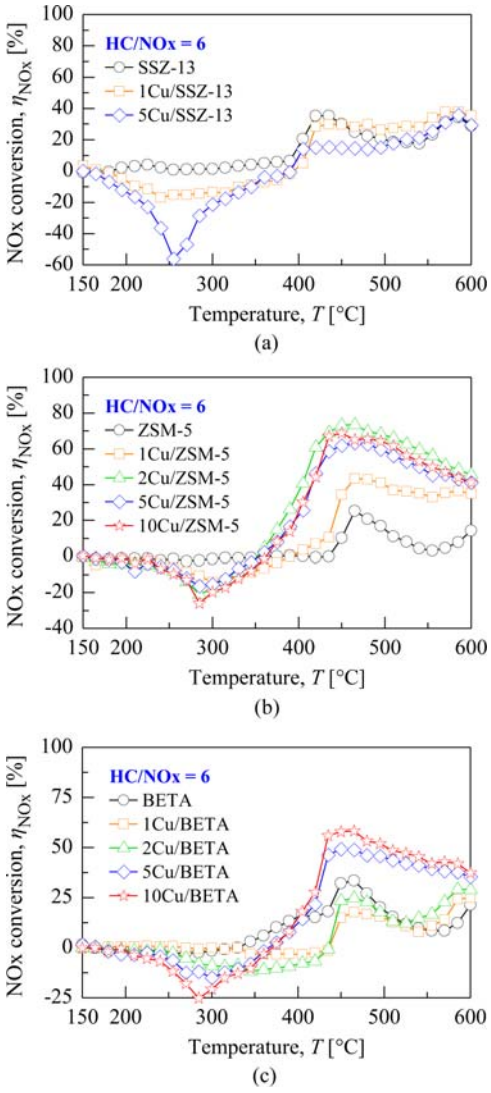

Figure 19. NOx conversion of Cu-based zeolites in SCR with C_4H_{10} as a function of reaction temperature; (a) Cu/SSZ-13, (b) Cu/ZSM-5, and (c) Cu/BETA. Feed conditions: 300 ppm NO, 500 ppm CO, 10 % CO_2, 5 % H_2O, 8 % O_2, 1800 ppmC_1 *n*-C_4H_{10} at GHSV = 12,500 h^{-1}. Reprinted with permission from Ref. (Lee *et al*., 2019a).

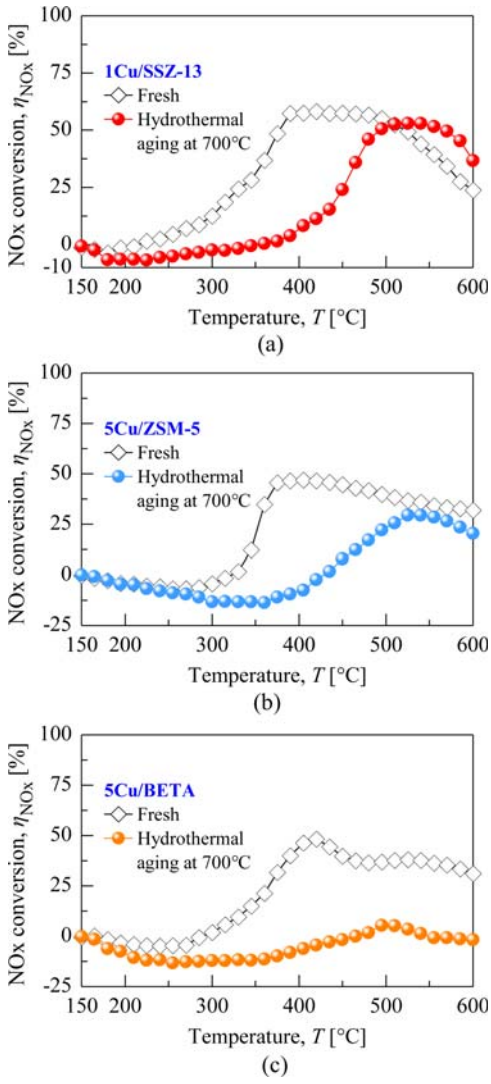

Figure 20. SCR performance of Cu/zeolite catalysts before and after 700 °C hydrothermal aging for 12 h (aging conditions: 5 % H_2O + 8 % O_2 + balance N_2 at GHSV = 12,500 h^{-1}). Feed conditions: 500 ppm NO, 500 ppm CO, 10 % CO_2, 5% H_2O, 8 % O_2, 4000 ppmC_1 C_3H_6 at GHSV = 12,500 h^{-1}. Reprinted with permission from Ref. (Lee *et al*., 2019b).

in Figure 20, the hydrothermally aged 5Cu/ZSM-5 and 5Cu/BETA catalysts exhibit a significant drop in the maximum NOx conversion compared to 1Cu/SSZ-13. The decreased HC-SCR performance could be attributed to the inhibition of the partial oxidation of the reducing agent during the HC-SCR process (Lee *et al*., 2019b). The catalytic activity of HC-SCR is also affected by the chemical properties of the HC species, such as the carbon-number, chain-length, chemical properties, etc. There have been attempts to evaluate various HC species and their related reaction mechanisms and further improve the SCR performance of the HC-SCR catalysts, particularly over the Cu/ZSM-5 and Fe/ZSM-5 catalysts, as summarized in Table 2. In the HC-SCR process, the carbon-carbon bonds of the reducing agent were indispensable for the HC-SCR reaction; they represented the chemical structure of the HC after the reaction (Erkfeldt *et al*., 2011).

In recent years, silver as a metal oxide catalyst impregnated on the γ-Al_2O_3 support (Ag/Al_2O_3) has attracted attention owing to its good SCR activity, sulfur tolerance, and hydrothermal stability (Chansai *et al*., 2014; Deng *et al*., 2016; Xu *et al*., 2019). To overcome the low-temperature catalytic activity of Ag/Al_2O_3, studies have been conducted for the improvement of the de-NOx performance at low temperatures by hydrogen addition in

Table 2. HC-SCR catalysts with various active phases and supports.

Support	Active metal	Reference
Ion-exchanged metal-based zeolite		
MOR	Ag	Shibata *et al*., 2004
	In	Berndt *et al*., 2003
SSZ-13	Cu	Lee *et al*., 2019a
ZSM-5	Mn	Aylor *et al*., 1997
	Cu	Lee *et al*., 2019b
BEA	Co	Sazama *et al*., 2015
Precious group metal (PGM) supported on metal oxide		
TiO_2	Au	Nguyen *et al*., 2009
$CeZrO_2$	Pd	Azambre *et al*., 2011
γ-Al_2O_3	Pt	Kim *et al*., 2012b

the feed stream, and the modification of the active phases (using metallic additives). Numerous efforts have been devoted to understanding the promotional effect of coexistent H_2 on NOx reduction by the HC-SCR process in the feed stream. The effect of H_2 on Ag/Al_2O_3 was first reported by Satokawa (2000), who highlighted that the catalytic activity of Ag/Al_2O_3 was significantly improved by adding H_2 in the presence of excess O_2 and H_2O. As illustrated in Figure 21, the maximum NOx conversion of Ag/Al_2O_3 was approximately 45 % at 780 K. However, the NOx conversion at low temperatures was significantly enhanced in the presence of H_2. Since the discovery of the H_2 effect, the NOx reduction of the HC-SCR was extensively evaluated over the Ag/Al_2O_3 catalyst in terms of, sulfur tolerance (Xu *et al*., 2019), water tolerance (Xu *et al*., 2018), metallic additives such as Au (More *et al*., 2015), optimization of Ag loading (Kim *et al*., 2013; Chaieb *et al*., 2014), and the promotional effect of coexistent CO (Shang *et al*., 2017).

Furthermore, many preparation methods have been attempted to design highly efficient Ag/Al_2O_3 catalysts for practical application in the HC-SCR system; for example, wet impregnation (Deng *et al*., 2015; Azizi *et al*., 2016), sol-gel synthesis (Seker *et al*., 1999; Azis *et al*., 2015), co-precipitation (Keshavaraja *et al*., 2000), and ball-milling (Kamolphop *et al*., 2011; Deng *et al*., 2016). Although the preparation of Ag/Al_2O_3 is still under investigation, wet impregnation from the aqueous solution with the $AgNO_3$ precursor, and the solvent-free ball-milling process have been recognized as the best preparation methods, owing to the high catalytic activity of the resulting Ag/Al_2O_3 catalysts (Kamolphop *et al*., 2011; Ralphs *et al*., 2014).

Major precious metals like Pt, Pd and Rh are very strong active catalysts with high thermal durability for the commercial application of the HC-SCR system. Because

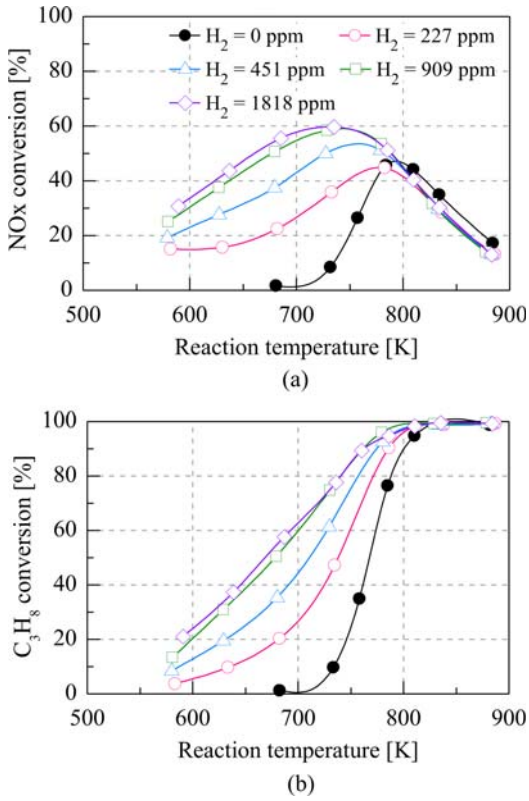

Figure 21. Effect of coexistent H_2 concentrations on NOx and C_3H_8 conversion over Ag/Al_2O_3 catalysts. Feed conditions: 91 ppm NO, 91 ppm C_3H_8, 9.1 % O_2, 9.1 % H_2O, and 0–1818 ppm H_2 at GHSV = 44,000 h^{-1} (Satokawa, 2000).

Ag, Co and Cu show high performance at low temperatures, these materials are being studied widely with efforts of overcoming high temperature durability. As an example, Ag can be used with Pt and Rh to enhance their low-temperature activity and provide aging temperature tolerances of Ag by Pt/Rh.

4.3. Reaction Mechanisms

The reaction mechanism of HC-SCR has been under debate for the past decades. Although, some reaction mechanisms have been elucidated, general reaction mechanisms are not available owing to the different catalyst types, reaction conditions, and numerous HC species. De-NOx activity and related reaction pathways were evaluated over the Cu ion-exchanged ZSM-5 in the presence of HCs and CO in the feed stream. The relevant reaction pathway of HC-SCR is shown in the following steps:

$$NO + CO + O_2 \rightarrow N_2 + CO_2 \quad (20)$$

$$NO + HC + O_2 \rightarrow N_2 + CO + H_2O \quad (21)$$

$$HC + NOx \rightarrow N_2 + CO_2 + H_2O \quad (22)$$

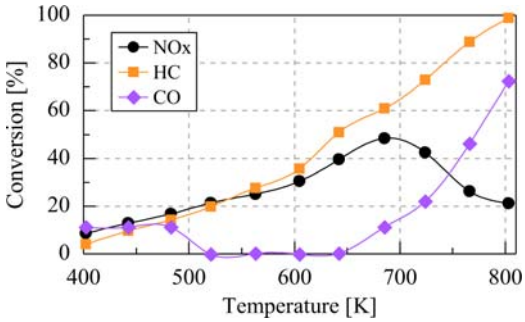

Figure 22. HC-SCR performance and proposed reaction pathway over Cu/ZSM-5. Feed conditions: 550 ppm NOx, 134 ppm HC, 0.11 % CO, A/F = 21 at GHSV = 25,000 h^{-1}. Reprinted with permission from Ref. (Landong *et al*., 2005).

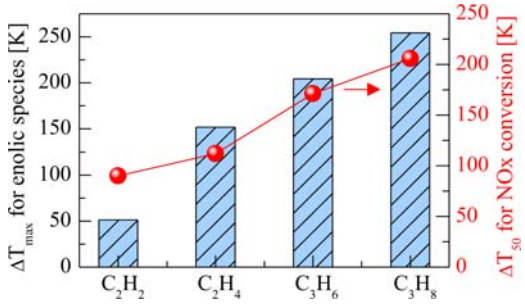

Figure 23. Relation between the ΔT_{max} for enolic species triggered by H_2 addition and ΔT_{50} for NOx conversion during HC-SCR process. Reprinted with permission from Ref. (Yu *et al*., 2014).

As illustrated in Figure 22, reactions (20) and (21) are the primary reactions of the NOx reduction at 400 ~ 500 K. In reaction (20), NO is reduced by CO, and slows the rate of reaction (21); NO is then reduced by HC and increases at temperatures above 500 K, because the CO conversion suddenly decreases from 500 K. These results indicate that the reaction mechanism of HC-SCR highly depends on the reaction temperatures. When the reaction temperature increases above 650 K, the primary reaction of the NOx reduction shifts from reaction (21) to reaction (22) because the CO conversion begins to increase; this is related to the consumption of CO as a reductant. The overall reaction pathway is that the NOx and HC species (CxHyOz) are simultaneously formed on the surface-activating sites; these species are the two significant reaction intermediates in the HC-SCR process (Landong *et al*., 2005).

In the case of the transitional metals over the metal oxide support, nitrogen-containing species, such as R–NH_2, –NCO, and NH_3 are formed via the organo-nitrogen species (Haneda *et al*., 1998). The reaction of NO with O_2 or HCs to form the ad-NOx species, and partially oxidized HCs (CxHyOz) are considered the crucial reaction intermediates during the HC-SCR process (Meunier *et al*., 2000). Several researchers have proposed the reaction mechanism in which the nitrogen-containing species (e.g. –NCO, R–NH_2, and NH_3) reacts with the oxidized nitrogen species (e.g. organo-nitrito or NO_2) to form N_2 (Sumiya *et al*., 1998; Kameoka *et al*., 1998).

Although some studies have been conducted using kinetic and spectroscopic evaluations to understand the HC-SCR process over the Cu/ZSM-5 catalysts, many aspects are still unclear. The possible reaction mechanism of the HC-SCR process over the ion-exchanged Cu/ZSM-5 was proposed, where allyl (CH_2=CH–CH_2–), allyl oxime (R_2–C=N–OH), ethenyl isocyanate (CH_2=CH–NCO), and ethenyl amine (CH_2=CH–NH_2) species participated in the NOx reduction as reaction intermediates (Park *et al*., 2000a). For the active sites, Park *et al*. (2000b) proposed Cu(I) and Cu(II) as the possible active sites of the redox cycles for NO decomposition over the dehydrated Cu(II)-exchanged ZSM-5. They proposed that Cu(II)–O^- reacts with NO to form Cu(I)–NO_2, the subsequent interaction of NO involves the formation of Cu(II)–(NO_2)(NO), and then Cu(I) reacts with NO to form Cu(I)–NO and Cu(I)–NO_2 of which the latter is transformed to Cu(II)–(N_2O)O^-. Therefore, Cu(I), Cu(II)–O^-, and paramagnetic Cu(II) are highly active species for NO adsorption, and they produce many Cu-NO complexes, which participate in the NOx reduction (Park *et al*., 2000b).

It has been accepted that the partial oxidation of HCs to active oxygenates, which is an initial step of the HC-SCR process, was promoted by adding H_2 at low temperatures over Ag/Al_2O_3, improving the NOx reduction (Bentrup *et al*., 2005; Zhang *et al*., 2007). Yu *et al*. (2014) evaluated the catalytic activity of Ag/Al_2O_3 in the H_2-assisted HC-SCR process using in situ DRIFTS (Yu *et al*., 2014). A variety of HCs (CH_4, C_2H_2, C_2H_4, C_3H_6, and C_3H_8) were tested, and two- or three-carbon atoms clearly improved the low-temperature de-NOx activity by H_2, whereas CH_4-SCR did not occur. They demonstrated the formation of enolic species (RCH=CH–O^-) during the partial oxidation of C_2H_2, C_2H_4, C_3H_6, and C_3H_8, particularly at low temperatures of 423 ~ 523 K. Therefore, the stronger the enolic species formation, the higher the catalytic activity for NOx reduction, as illustrated in Figure 23.

5. H_2/CO-SCR TECHNOLOGY

Compared with the current urea-SCR, the SCR of NOx with H_2 in the presence of O_2 (H_2-SCR) has attracted considerable attention owing to the absence of pollutants (Hu *et al*., 2020). With respect to the previous two SCR systems (urea-SCR and HC-SCR), H_2-SCR is an environmentally friendly technology because it can not only reduce NOx at relatively low temperatures (< 200 °C) (Wang *et al*., 2016), but also reduce CO_2 emission (a greenhouse gas), which is a drawback of the HC-SCR system. The H_2 is produced by reforming the diesel fuel

(Savva and Costa, 2011) and the WGS reaction (Hu and Yang, 2019). Numerous studies have been conducted using noble-metal catalysts in the H_2-SCR process, especially for Pd (Zhang *et al*., 2019b) and Pt (Wang *et al*., 2019b) catalysts, which have been recognized as the active phases. NO is first adsorbed molecularly or dissociatively onto the surface of the noble metal, depending on the surface properties. The dissociated NO forms reaction intermediates with the adsorbed H_2 and follow the reaction pathway of NO + H → NH + O, which is the most conducive for N_2 formation because of the lower reaction energy barrier (Patel and Sharma, 2020). Therefore, active phases with excellent de-NOx performance at low temperatures in the H_2-SCR process are identified. Various reaction mechanisms have been proposed in the literature (Frank *et al*., 1998; Costa and Efstathiou, 2007; Zhao *et al*., 2015; Komatsubara *et al*., 2016; Hong *et al*., 2018).

As one of the contaminants in the combustion process, carbon monoxide (CO) is more attractive in a practical point of view. The SCR of NO by CO (CO-SCR) exhibits good reducing effects of NOx to produce N_2 and CO_2. NOx and CO can be simultaneously reduced in the CO-SCR process, and CO is considerably cheaper and easily available (Zhang *et al*., 2020). The active catalysts used in the CO-SCR process, including Pd, Pt, or Rh-based catalysts, have little catalytic activity (Wang *et al*., 2003; Hamada and Haneda, 2012), whereas Ag and Ir-based catalysts exhibit a reasonably high de-NOx performance in the presence of O_2 at temperature ranging from 250 ~ 450 °C (Takahashi *et al*., 2006; Wu *et al*., 2016). The catalytic activity of CO-SCR shows a strong inhibitory effect in the presence of O_2, owing to the competitive reaction of CO between O_2 and NOx, resulting in a severe decrease in the de-NOx performance (Sreekanth and Smirniotis, 2008; Yamamoto *et al*., 2002a; Yamamoto *et al*., 2002b). Consequently, many studies have examined the CO-SCR process in the absence of O_2 (Sun *et al*., 2017; Liu *et al*., 2017b; Shi *et al*., 2018; Oton *et al*., 2020), where the absence of O_2 in the feed stream is far from actual diesel exhaust conditions. Recently, Ce-modified Cu-BTC catalysts for the CO-SCR reaction have been reported. These catalysts exhibit complete NO conversion below 300 °C in the presence of 5 vol% O_2 (Zhang *et al*., 2020). Similarly, bimetallic Ir and Ru supported on Al_2O_3 catalysts ($IrRu/Al_2O_3$) exhibit a reasonable de-NOx performance in the presence of excessive O_2 (> 5 %) at low temperatures (Song *et al*., 2020; Heo *et al*., 2020).

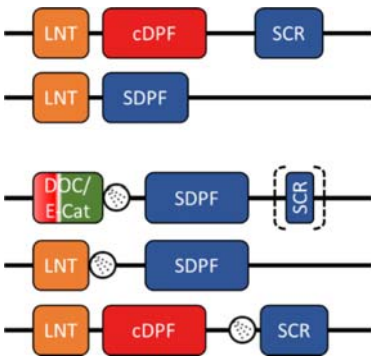

Figure 24. Suggesting after-treatment systems for diesel vehicles (Ruwisch, 2015).

6. CONCLUSION

To meet the stricter emission standards for diesel engines such as Euro 7/RDE, it is necessary to use a combination of the various after-treatment technologies discussed above. Currently, various technologies such as the LNT, SCR, SDPF, and CDPF are applied in diesel vehicles. As shown in Figure 24, actual examples of the Umicore after-treatment system arrangement according to the displacement of the diesel engine have been proposed. The exhaust after-treatment system of the diesel vehicle essentially uses a combination of LNT and SCR (or SDPF). In the case of heavy-duty diesel vehicles, an electrically heated catalyst (E-CAT), which is technology from the 1990s that heats exhaust gases during a cold start, has been proposed. As discussed above, the after-treatment technology of diesel vehicles in the future will be categorized into various methods, in which conventional and newly advanced technology are combined. Because diesel emissions include HCs, CO, and NOx as gaseous components, and PM as solid components in lean atmospheres as described above, the after-treatment system includes various technologies, which causes a huge burden in terms of cost and space for installation. Further, it is critical to develop suitable control algorithms and measures for the various de-NOx technologies at wide temperature windows under dynamic operating conditions to achieve compliance with very strict legislation requirements. The limitations of cost and installation space with the control complexities of diesel vehicles will be the key factors for the advancement of de-NOx technology in the future and allow these vehicles to compete with vehicles employing traditional powertrains, like gasoline vehicles, and the latest electric vehicles.

ACKNOWLEDGEMENT–This research was supported by Technology Development Program to Solve Climate Changes through the National Research Foundation of Korea (NRF) funded by the Ministry of Science, ICT (2019M1A2A2104052).

REFERENCES

Arai, H., Yamada, T., Eguchi, K. and Seiyama, T. (1986). Catalytic combustion of methane over various perovskite-type oxides. *Applied Catalysis* **26**, 265–276.

Auvray, X., Grant, A., Lundberg, B. and Olsson, L. (2019). Lean and rich aging of a Cu/SSZ-13 catalyst for combined lean NOx trap (LNT) and selective catalytic

reduction (SCR) concept. *Catalysis Science & Technology* **9**, **9**, 2152–2162.

Aylor, A. W., Lobree, L. J., Reimer, J. A. and Bell, A. T. (1997). NO adsorption, desorption, and reduction by CH_4 over Mn-ZSM-5. *J. Catalysis* **170**, **2**, 390–401.

Azambre, B., Zenboury, L., Da Costa, P., Capela, S., Carpentier, S. and Westermann, A. (2011). Palladium catalysts supported on sulfated ceria–zirconia for the selective catalytic reduction of NOx by methane: Catalytic performances and nature of active Pd species. *Catalysis Today* **176**, **1**, 242–249.

Azis, M. M., Härelind, H. and Creaser, D. (2015). On the role of H_2 to modify surface NOx species over Ag–Al_2O_3 as lean NOx reduction catalyst: TPD and DRIFTS studies. *Catalysis Science & Technology* **5**, **1**, 296–309.

Azizi, Y., Kambolis, A., Boréave, A., Giroir-Fendler, A., Retailleau-Mevel, L., Guiot, B., Marchand, O., Walter, M., Desse, M.-L., Marchin, L. and Vernoux, P. (2016). NOx abatement in the exhaust of lean-burn natural gas engines over Ag-supported γ-Al_2O_3 catalysts. *Surface Science*, **646**, 186–193.

Bentrup, U., Richter, M. and Fricke, R. (2005). Effect of H_2 admixture on the adsorption of NO, NO_2 and propane at Ag/Al_2O_3 catalyst as examined by in situ FTIR. *Applied Catalysis B: Environ*mental **55**, **3**, 213–220.

Berndt, H., Schütze, F.-W., Richter, M., Sowade, T. and Grünert, W. (2003). Selective catalytic reduction of NO under lean conditions by methane and propane over indium/cerium-promoted zeolites. *Applied Catalysis B: Environmental* **40**, **1**, 51–67.

Burch, R. and Watling, T. C. (1997). The difference between alkanes and alkenes in the reduction of NO by hydrocarbons over Pt catalysts under lean-burn conditions. *Catalysis Letters* **43**, **1-2**, 19–23.

Burch, R., Millington, P. J. and Walker, A. P. (1994). Mechanism of the selective reduction of nitrogen monoxide on platinum-based catalysts in the presence of excess oxygen. *Applied Catalysis B: Environmental* **4**, **1**, 65–94.

Castoldi, L., Lietti, L., Forzatti, P., Morandi, S., Ghiotti, G. and Vindigni, F. (2010). The NOx storage-reduction on Pt-K/Al_2O_3 Lean NOx Trap catalyst. *J. Catalysis* **276**, **2**, 335-350.

Cha, W., Ehrman, S. H. and Jurng, J. (2016). CeO_2 added V_2O_5/TiO_2 catalyst prepared by chemical vapor condensation (CVC) and impregnation method for enhanced NH_3-SCR of NOx at low temperature. *J. Environmental Chemical Engineering* **4**, **1**, 556–563.

Chaieb, T., Delannoy, L., Costentin, G., Louis, C., Casale, S., Chantry, R. L. and Thomas, C. (2014). Insights into the influence of the Ag loading on Al_2O_3 in the H_2-assisted C_3H_6-SCR of NOx. *Applied Catalysis B: Environmental*, **156–157**, 192–201.

Chansai, S., Burch, R., Hardacre, C., Norton, D., Bao, X. and Lewis, L. (2014). Investigating the promotional effect of methanol on the low temperature SCR reaction on Ag/Al_2O_3. *Applied Catalysis B: Environmental*, **160–161**, 356–364.

Chaugule, S. S., Yezerets, A., Currier, N. W., Ribeiro, F. H. and Delgass, W. N. (2010). 'Fast' NOx storage on Pt/BaO/γ-Al_2O_3 Lean NOx Traps with NO_2 + O_2 and NO + O_2: Effects of Pt, Ba loading. *Catalysis Today* **151**, **3–4**, 291–303.

Cheng, X. and Bi, X. T. (2014). A review of recent advances in selective catalytic NOx reduction reactor technologies. *Particuology*, **16**, 1–18.

Choi, B. and Lee, K.-S. (2014). LNT/CDPF catalysts for simultaneous removal of NOx and PM from diesel vehicle exhaust. *Chemical Engineering J.*, **240**, 476–486.

Choi, J. S., Partridge, W. P. and Daw, C. S. (2007). Sulfur impact on NOx storage, oxygen storage, and ammonia breakthrough during cyclic lean/rich operation of a commercial lean NOx trap. *Applied Catalysis B: Environmental* **77**, **1–2**, 145–156.

Choi, J. S., Partridge, W. P., Pihl, J. A. and Daw, C. S. (2008). Sulfur and temperature effects on the spatial distribution of reactions inside a lean NOx trap and resulting changes in global performance. *Catalysis Today* **136**, **1–2**, 173–182.

Constantinou, C., Li, W., Qi, G. and Epling, W. S. (2013). NOx storage and reduction over a perovskite-based lean NOX trap catalyst. *Applied Catalysis B: Environmental,* **134–135**, 66–74.

Costa, C. N. and Efstathiou, A. M. (2007). Mechanistic aspects of the H_2-SCR of NO on a novel Pt/MgO−CeO_2 catalyst. *J. Physical Chemistry C* **111**, **7**, 3010–3020.

Cui, Y., Wang, Y., Mei, D., Walter, E. D., Washton, N. M., Holladay, J. D., Wang, Y., Szanyi, J., Peden, C. H. F. and Gao, F. (2019). Revisiting effects of alkali metal and alkaline earth co-cation additives to Cu/SSZ-13 selective catalytic reduction catalysts. *J. Catalysis*, **378**, 363–375.

Deka, U., Lezcano-Gonzalez, I., Warrender, S. J., Picone, A. L., Wright, P. A., Weckhuysen, B. M. and Beale, A. M. (2013). Changing active sites in Cu–CHA catalysts: deNOx selectivity as a function of the preparation method. *Microporous Mesoporous Materials*, **166**, 144–152.

Deng, H., Yu, Y. and He, H. (2015). Discerning the role of Ag–O–Al entities on Ag/γ-Al_2O_3 surface in NOx selective reduction by ethanol. *J. Physical Chemistry C* **119**, **6**, 3132–3142.

Deng, H., Yu, Y. and He, H. (2016). Water effect on preparation of Ag/Al_2O_3 catalyst for reduction of NOx by ethanol. *J. Physical Chemistry C* **120**, **42**, 24294–24301.

Descorme, C., Gélin, P., Primet, M. and Lécuyer, C. (1996). Infrared study of nitrogen monoxide adsorption on palladium ion-exchanged ZSM-5 catalysts. *Catalysis Letters* **41**, **3-4**, 133–138.

Erkfeldt, S., Palmqvist, A. and Petersson, M. (2011). Influence of the reducing agent for lean NOx reduction

over Cu-ZSM-5. *Applied Cataysis B: Environmental* **102**, **3–4**, 547–554.

Fan, C., Chen, Z., Pang, L., Ming, S., Zhang, X., Albert, K. B., Liu, P., Chen, H. and Li, T. (2018). The influence of Si/Al ratio on the catalytic property and hydrothermal stability of Cu-SSZ-13 catalysts for NH_3-SCR. *Applied Catalysis A: General*, **550**, **3–4**, 256-265.

Feng, X., Cao, Y., Lan, L., Lin, C., Li, Y., Xu, H., Gong, M. and Chen, Y. (2016). The promotional effect of Ce on CuFe/beta monolith catalyst for selective catalytic reduction of NOx by ammonia. *Chemical Engineering J.*, **302**, 697–706.

Frank, B., Emig, G. and Renken, A. (1998). Kinetics and mechanism of the reduction of nitric oxides by H_2 under lean-burn conditions on a Pt–Mo–Co/α-Al_2O_3 catalyst. *Applied Catalysis B: Environmental* **19**, **1**, 45–57.

Gao, F. and Szanyi, J. (2018). On the hydrothermal stability of Cu/SSZ-13 SCR catalysts. *Applied Catalysis A: General*, **560**, 185–194.

Hamada, H. and Haneda, M., (2012). A review of selective catalytic reduction of nitrogen oxides with hydrogen and carbon monoxide. *Applied Catalysis A: General*, **421–422**, 1–13.

Han, J., Kim, T., Jung, H., Pyo, S., Cho, G., Oh, Y. and Kim, H. (2019). Improvement of NOx reduction rate of urea SCR system applied for an non-road diesel engine. *Int. J. Automotive Technology* **20**, **6**, 1153−1160.

Haneda, M., Kintaich, Y., Inaba, M. and Hamada, H. (1998). Infrared study of catalytic reduction of nitrogen monoxide by propene over Ag/TiO_2–ZrO_2. *Catalysis Today* **42**, **1–2**, 127–135.

Held, W., König, A., Richter, T. and Puppe, L. (1990). Catalytic NOx reduction in net oxidizing exhaust gas. *SAE Paper No.* 900496.

Heo, I., You, Y. W., Lee, J. H., Schmieg, S. J., Yoon, D. Y. and Kim, C. H. (2020). Urealess NOx reduction by carbon monoxide in simulated lean-burn exhausts. *Environmental Science Technology* **54**, **13**, 8344–8351.

Hong, Z., Wang, Z., Chen, D., Sun, Q. and Li, X. (2018). Hollow ZSM-5 encapsulated Pt nanoparticles for selective catalytic reduction of NO by hydrogen. *Applied Surface Science*, **440**, 1037–1046.

Hu, Z. and Yang, R. T. (2019). 110th Anniversary: Recent progress and future challenges in selective catalytic reduction of NO by H_2 in the presence of O_2. *Industrial & Engineering Chemistry Research* **58**, **24**, 10140–10153.

Hu, Z., Yong, X., Li, D. and Yang, R. T. (2020). Synergism between palladium and nickel on Pd-Ni/TiO_2 for H_2-SCR: A transient DRIFTS study. *J. Catalysis*, **381**, 204–214.

Iwamoto, M., Yahiro, H., Tanda, K., Mizuno, N., Mine, Y. and Kagawa, S. (1991). Removal of nitrogen monoxide through a novel catalytic process. 1. Decomposition on excessively copper-ion-exchanged ZSM-5 zeolites. *J. Physical Chemistry* **95**, **9**, 3727–3730.

Iwamoto, M., Yahiro, H., Yuu, Y., Shundo, S. and Mizuno, N. (1990). Selective reduction of NO by lower hydrocarbons in the presence of O_2 and SO_2 over copper ion-exchanged zeolites. *Shokubai*, **32**, 430–433.

Ji, Y., Choi, J. S., Toops, T. J., Crocker, M. and Naseri, M. (2008). Influence of ceria on the NOx storage/reduction behavior of lean NOx trap catalysts. *Catalysis Today* **136**, **1-2**, 146–155.

Ji, Y., Easterling, V., Graham, U., Fisk, C., Crocker, M. and Choi, J. S. (2011). Effect of aging on the NOx storage and regeneration characteristics of fully formulated lean NOx trap catalysts. *Applied Catalysis B: Environmental* **103**, **3–4**, 413–427.

Jung, Y., Shin, Y. J., Pyo, Y. D., Cho, C. P., Jang, J. and Kim, G. (2017). NOx and N_2O emissions over a Urea-SCR system containing both V_2O_5-WO_3/TiO_2 and Cu-zeolite catalysts in a diesel engine. *Chemical Engineering J.*, **326**, 853–862.

Kameoka, S., Chafik, T., Ukisu, Y. and Miyadera, T. (1998). Reactivity of surface isocyanate species with NO, O_2 and NO+O_2 in selective reduction of NOx over Ag/Al_2O_3 and Al_2O_3 catalysts. *Catalysis Letters* **55**, **3-4**, 211–215.

Kamolphop, U., Taylor, S. F. R., Breen, J. P., Burch, R., Delgado, J. J., Chansai, S., Hardacre, C., Hengrasmee, S. and James, S. L. (2011). Low-temperature Selective Catalytic Reduction (SCR) of NOx with n-Octane using solvent-free mechanochemically prepared Ag/Al_2O_3 catalysts. *ACS Catalysis* **1**, **10**, 1257–1262.

Kang, W., Choi, B., Jung, S. and Park, S. (2018). PM and NOx reduction characteristics of LNT/DPF+SCR/DPF hybrid system. *Energy* **143**, 439–447.

Keshavaraja, A., She, X. and Flytzani-Stephanopoulos, M. (2000). Selective catalytic reduction of NO with methane over Ag-alumina catalysts. *Applied Catalysis B: Environmental* **27**, **1**, L1–L9.

Kim, B. S., Jeong, H., Bae, J., Kim, P. S., Kim, C. H. and Lee, H. (2020). Lean NOx trap catalysts with high low-temperature activity and hydrothermal stability. *Applied Catalysis B: Environmental,* **270**, 118871.

Kim, C. H., Qi, G., Dahlgerg, K. and Li, W. (2010). Strontium-doped perovskites rival platinum catalysts for treating NOx in simulated diesel exhaust. *Science* **327**, **5973**, 1624–1627.

Kim, D. H., Mudiyanselage, K., Szanyi, J., Zhu, H., Kwak, J. H. and Peden, C. H. F. (2012a). Characteristics of Pt–K/$MgAl_2O_4$ lean NOx trap catalysts. *Catalysis Today* **184**, **1**, 2–7.

Kim, P. S., Kim, M. K., Cho, B. K., Nam, I.-S. and Oh, S. H. (2013). Effect of H_2 on deNOx performance of HC-SCR over Ag/Al_2O_3: Morphological, chemical, and kinetic changes. *J. Catalysis*, **301**, 65–76.

Kim, S. S., Choi, S. H., Lee, S. M. and Hong, S. C. (2012b). Enhanced catalytic activity of Pt/Al_2O_3 on the CH_4 SCR. *J. Industrial Engineering Chemistry* **18**, **1**, 272–276.

Koebel, M., Elsener, M. and Kleemann, M. (2000). Urea-SCR: a promising technique to reduce NOx emissions from automotive diesel engines. *Catalysis Today* **59**, **3–4**, 335–345.

Koebel, M., Elsener, M. and Marti, T. (1996). NOx-reduction in diesel exhaust gas with urea and selective catalytic reduction. *Combustion Science Technology* **121**, **1–6**, 85–102.

Komatsubara, M., Koga, A., Tanaka, M., Hagiwara, R. and Iwamoto, M. (2016). Three pathways to selective catalytic reduction of NO over Pt/Nb-AlMCM-41 under H_2 with excess O_2. *Catalysis Science Technology* **6**, **20**, 7398–7407.

Kröcher, O. (2007). Aspects of catalyst development for mobile urea-SCR systems — From Vanadia-Titania catalysts to metal-exchanged zeolites. *Studies Surface Science and Cataysis*, **171**, 261–289.

Kwak, J. H., Kim, D. H., Szanyi, J. and Peden, C. H. F. (2008). Excellent sulfur resistance of Pt/BaO/CeO_2 lean NOx trap catalysts. *Applied Catalysis B: Environmental* **84**, **3–4**, 545–551.

Landong, L., Jixin, C., Shujuan, Z., Fuxiang, Z., Naijia, G., Tianyou, W. and Shuliang, L. (2005). Selective catalytic reduction of nitrogen oxides from exhaust of lean burn engine over in-situ synthesized Cu−ZSM-5/cordierite. *Environmental Science and Technology* **39**, **8**, 2841–2847.

Lee, K., Choi, B., Lee, C. and Oh, K. (2020). Effects of SiO_2/Al_2O_3 ratio, reaction atmosphere and metal additive on de-NOx performance of HC-SCR over Cu-based ZSM-5. *J. Industrial Engineering Chem*istry, **90**, 132–144.

Lee, K., Kosaka, H., Sato, S., Yokoi, T. and Choi, B. (2019a). Effect of Cu content and zeolite framework of *n*-C_4H_{10}-SCR catalysts on de-NOx performances. *Chemical Engineering Science*, **203**, 28–42.

Lee, K., Kosaka, H., Sato, S., Yokoi, T., Choi, B. and Kim, D. (2019b). Effects of Cu loading and zeolite topology on the selective catalytic reduction with C_3H_6 over Cu/zeolite catalysts. *J. Industrial Engineering Chemistry*, **72**, 73–86.

Liu, L., Wu, X., Ma, Y., Zhang, X., Ran, R., Si, Z. and Weng, D. (2020). Potassium deactivation of Cu-SSZ-13 catalyst for NH_3-SCR: Evolution of salts, zeolite and copper species. *Chemical Engineering J*., **383**, 123080.

Liu, Q., Fu, Z., Ma, L., Niu, H., Liu, C., Li, J. and Zhang, Z. (2017a). MnOx-CeO_2 supported on Cu-SSZ-13: A novel SCR catalyst in a wide temperature range. *Applied Catalysis A:General*, **547**, 146–154.

Liu, T., Qian, J., Yao, Y., Shi, Z., Han, L., Liang, C., Li, B., Dong, L., Fan, M. and Zhang, L. (2017b). Research on SCR of NO with CO over the $Cu_{0.1}La_{0.1}Ce_{0.8}O$ mixed-oxide catalysts: Effect of the grinding. *Molecular Catalysis*, **430**, 43–53.

Luo, J.-Y., Oh, H., Henry, C. and Epling, W. (2012). Effect of C_3H_6 on selective catalytic reduction of NOx by NH_3 over a Cu/zeolite catalyst: A mechanistic study. *Applied Catalysis B:Environmental*, **123–124**, 296–305.

Lv, L., Wang, X., Shen, M., Zhang, Q. and Wang, J. (2013). The lean NOx traps behavior of (1–5 %) BaO/CeO_2 mixed with Pt/Al_2O_3 at low temperature (100–300 °C): The effect of barium dispersion. *Chemical Engineering J*., **222**, 401–410.

Ma, L., Su, W., Li, Z., Li, J., Fu, L. and Hao, J. (2015). Mechanism of propene poisoning on Cu-SSZ-13 catalysts for SCR of NOx with NH_3. *Catalysis Today*, **245**, 16–21.

Matsumoto, S., Ikeda, Y., Suzuki, H., Ogai, M. and Miyoshi, N. (2000). NOx storage-reduction catalyst for automotive exhaust with improved tolerance against sulfur poisoning. *Applied Catalysis B: Environmental* **25**, **2–3**, 115–124.

Meunier, F. C., Zuzaniuk, V., Breen, J. P., Olsson, M. and Ross, J. R. H. (2000). Mechanistic differences in the selective reduction of NO by propene over cobalt- and silver-promoted alumina catalysts: kinetic and in situ DRIFTS study. *Catalysis Today* **59**, **3–4**, 287–304.

Miller, J. T., Glusker, E., Peddi, R., Zheng, T. and Regalbuto, J. R. (1998). The role of acid sites in cobalt zeolite catalysts for selective catalytic reduction of NOx. *Catalysis Letters* **51**, **1-2**, 15–22.

Mohan, S., Dinesha, P. and Kumar, S. (2020). NOx reduction behaviour in copper zeolite catalysts for ammonia SCR systems: A review. *Chemical Engineering J*., **384**, 123253.

More, P. M., Nguyen, D. L., Granger, P., Dujardin, C., Dongare, M. K. and Umbarkar, S. B. (2015). Activation by pretreatment of Ag–Au/Al_2O_3 bimetallic catalyst to improve low temperature HC-SCR of NOx for lean burn engine exhaust. *Applied Catalysis B: Environmental,* **174–175**, 145–156.

Morita, T., Suzuki, N., Satoh, N., Wada, K. and Ohno, H. (2007). Study on low NOx emission control using newly developed lean NOx catalyst for diesel engines. *SAE Paper No.* 2007-01-0239.

Nguyen, L. Q., Salim, C. and Hinode, H. (2009). Promotive effect of MOx (M=Ce, Mn) mechanically mixed with Au/TiO_2 on the catalytic activity for nitrogen monoxide reduction by propene. *Topics Catalysis* **52**, **6-7**, 779–783.

Onrubia-Calvo, J. A., Pereda-Ayo, B., Caravaca, A. and De-La-Torre, U. (2020). Tailoring perovskite surface composition to design efficient lean NOx trap Pd–$La_{1-x}AxCoO_3/Al_2O_3$-type catalysts (with A=Sr or Ba). *Applied Catalysis B: Environmental*, **266**, 118628.

Oton, L. F., Oliveria, A. C., de Araujo, J. C. S., Araujo, R. S., de Sousa, F. F., Saravia, G. D., Lang, R., Otubo, L., da Silva Duarte, G. C. and Campos, A. (2020). Selective catalytic reduction of NOx by CO (CO-SCR) over metal-supported nanoparticles dispersed on porous alumina. *Advanced Powder Technology* **31**, **1**, 464–476.

Ottinger, N. A., Toops, T. J., Nguyen, K., Bunting, B. G.

and Howe, J. (2011). Effect of lean/rich high temperature aging on NO oxidation and NOx storage/release of a fully formulated lean NOx trap. *Applied Catalysis B: Environmental* **101**, **3–4**, 486–494.

Ottinger, N. A., Toops, T. J., Pihl, J. A., Roop, J. T., Choi, J. S. and Partridge, W. P. (2012). Sulfate storage and stability on representative commercial lean NOx trap components. *Applied Catalysis B: Environmental*, **117–118**, 167–176.

Pan, Y., Shen, B., Liu, L., Yao, Y., Gao, H., Liang, C. and Xu, H. (2020). Develop high efficient of NH_3-SCR catalysts with wide temperature range by ball-milled method. *Fuel*, **282**, 118834.

Park, S.-K., Kurshev, V., Luan, Z., Lee, C. W. and Kevan, L. (2000b). Reaction of NO with copper ions in Cu(II)-exchanged ZSM-5 zeolite: electron spin resonance, electron spin echo modulation and Fourier transform infrared spectroscopy. *Microporous Mesoporous Materials* **38**, **2–3**, 255–266.

Park, S.-K., Park, Y.-K., Park, S.-E. and Kevan, L. (2000a). Comparison of selective catalytic reduction of NO with C_3H_6 and C_3H_8 over Cu(II)-ZSM-5 and Co(II)-ZSM-5. *Physical Chemistry Chemical Physics* **2**, **23**, 5500–5509.

Park, S., Choi, B. and Oh, B. S. (2011). A combined system of dimethyl ether (DME) steam reforming and lean NOx trap catalysts to improve NOx reduction in DME engines. *Int. J. Hydrogen Energy* **36**, **11**, 6422–6432.

Park, S., Choi, B., Kim, H. and Kim, J.-H. (2012). Hydrogen production from dimethyl ether over Cu/γ-Al_2O_3 catalyst with zeolites and its effects in the lean NOx trap performance. *Int. J. Hydrogen Energy* **37**, **6**, 4762–4773.

Park, S., Oh, J. and Lee, K. (2018). Investigation on spray behavior and NOx conversion characteristic of a secondary injector for a lean NOx trap catalyst. *Int. J. Automotive Technol*ogy **19**, **2**, 199–207.

Patel, V. K. and Sharma, S. (2020). Effect of oxide supports on palladium based catalysts for NO reduction by H_2-SCR. *Catalysis Today.*

Peng, C., Liu, Z., Horimoto, A., Anand, C., Yamada, H., Ohara, K., Sukenaga, S., Ando, M., Shibata, H., Takewaki, T., Mukti, R.R., Okubo, T. and Wakihara, T. (2018). Preparation of nanosized SSZ-13 zeolite with enhanced hydrothermal stability by a two-stage synthetic method. *Microporous Mesoporous Materials,* **255**, 192–199.

Peng, C., Yan, R., Peng, H., Mi, Y., Liang, J., Liu, W., Wang, X., Song, G., Wu, P. and Liu, F. (2020). One-pot synthesis of layered mesoporous ZSM-5 plus Cu ion-exchange: Enhanced NH_3-SCR performance on Cu-ZSM-5 with hierarchical pore structures. *J. Hazard Materials,* **385**, 121593.

Peng, Y., Li, J., Huang, X., Li, X., Su, W., Sun, X., Wang, D. and Hao, J. (2014). Deactivation mechanism of potassium on the V_2O_5/CeO_2 catalysts for SCR reaction: acidity, reducibility and adsorbed-NOx. *Environmental Science Technology* **48**, **8**, 4515–4520.

Pieta, I. S., Epling, W. S., Garcia-Dieguez, M., Luo, J. Y., Larrubia, M. A., Herrera, M. C. and Alemany, L. J. (2011). Nanofibrous Pt-Ba Lean NOx trap catalyst with improved sulfur resistance and thermal durability. *Catalysis Today* **175**, **1**, 55–64.

Praveena, V. and Martin M. L. J. (2018). A review on various after treatment techniques to reduce NOx emissions in a CI engine. *J. Energy Institute* **91**, **5**, 704–720.

Ralphs, K., D'Agostino, C., Burch, R., Chansai, S., Gladden, L. F., Hardacre, C., James, S. L., Mitchell, J. and Taylor, S. F. R. (2014). Assessing the surface modifications following the mechanochemical preparation of a Ag/Al_2O_3 selective catalytic reduction catalyst. *Catalysis Science Technology* **4**, **2**, 531–539.

Reihani, A., Fisher, G. B., Hoard, J. W., Theis, J. R., Pakko, J. D. and Lambert, C. K. (2018). Rapidly pulsed reductants for diesel NOx reduction with lean NOx traps: Effects of pulsing parameters on performance. *Applied Catalysis B: Environmental*, **223**, 177–191.

Roy, S. and Baiker, A. (2009). NOx storage−reduction catalysis: from mechanism and materials properties to storage−reduction performance. *Chemical Reviews* **109**, **9**, 4054–4091.

Ruwisch, L. (2015). Trends & potentials of todays and future aftretreatment systems for diesel passenger vehicle. *2015 Int. Conf. Advanced Automotive Technology*, Gwangju, Korea.

Satokawa, S. (2000). Enhancing the NO/C3H8/O2 reaction by using H_2 over Ag/Al_2O_3 catalysts under lean-exhaust conditions. *Chemistry Letters* **29**, **3**, 294–295.

Savva, P. G. and Costa, C. N. (2011). Hydrogen lean-DeNOx as an alternative to the ammonia and hydrocarbon selective catalytic reduction (SCR). *Catalysis Reviews: Science and Engineering* **53**, **2**, 91–151.

Sazama, P., Mokrzycki, L., Wichterlova, B., Vondrova, A., Pilar, R., Dedecek, J., Sklenak, S. and Tabor, E. (2015). Unprecedented propane–SCR-NOx activity over template-free synthesized Al-rich Co-BEA* zeolite. *J. Catalysis*, **332**, 201–211.

Schaber, P. M., Colson, J., Higgins, S., Dietz, E., Thielen, D., Anspach, B. and Brauer, J. (1999). Study of the urea thermal decomposition (pyrolysis) reaction and importance to cyanuric acid production. *American Laboratory (Fairfield)* **31**, **16**, 13–21.

Seker, E., Cavataio, J., Gulari, E., Lorpongpaiboon, P. and Osuwan, S. (1999). Nitric oxide reduction by propene over silver/alumina and silver–gold/alumina catalysts: effect of preparation methods. *Applied Catalysis A: General* **183**, **1**, 121–134.

Seo, C.-K., Kim, H., Choi, B., Lim, M. T., Lee, C. H. and Lee, C.-B. (2011). De-NOx characteristics of a combined system of LNT and SCR catalysts according

to hydrothermal aging and sulfur poisoning. *Catalysis Today* **164**, **1**, 507–514.

Shan, Y., Sun, Y., Du, J., Zhang, Y., Shi, X., Yu, Y., Shan, W. and He, H. (2020). Hydrothermal aging alleviates the inhibition effects of NO_2 on Cu-SSZ-13 for NH_3-SCR. *Applied Catalysis B: Environmental*, **275**, 119105.

Shang, Z., Cao, J., Wang, L., Guo, Y., Lu, G. and Guo, Y. (2017). The study of C_3H_8-SCR on Ag/Al_2O_3 catalysts with the presence of CO. *Catalysis Today* **281**, **3**, 605–609.

Shi, X. Chu, B., Wang, F., Wei, X., Teng, L., Fan, M., Li, B., Dong, L. and Dong, L. (2018). Mn-modified CuO, $CuFe_2O_4$, and γ-Fe_2O_3 three-phase strong synergistic coexistence catalyst system for NO reduction by CO with a wider active window. *ACS Applied Materials & Interfaces* **10**, **47**, 40509–40522.

Shi, Y., Wang, X., Xia, Y., Sun, C., Zhao, C., Li, S. and Li, W. (2017). Promotional effect of CeO_2 on the propene poisoning resistance of HBEA zeolite catalyst for NH_3-SCR of NOx. *Molecular Catalysis*, **433**, 265–273.

Shibata, G., Eijima, W., Koiwai, R., Shimizu, K.-I., Nakasaka, Y., Kobashi, Y., Kubota, Y., Ogura, M. and Kusaka, J. (2019). NH_3-SCR by monolithic Cu-ZSM-5 and Cu-AFX catalysts: Kinetic modeling and engine bench tests. *Catalysis Today* **332**, 59–63.

Shibata, J., Takada, Y., Shichi, A., Satokawa, S., Satsuma, A. and Hattori, T. (2004). Influence of zeolite support on activity enhancement by addition of hydrogen for SCR of NO by propane over Ag-zeolites. *Applied Catalysis B: Environmental* **54**, **3**, 137–144.

Simböck, J., Khetan, A., Pegios, N., Iskandar, R., Schwedt, A., Harmsen, J. M. A., Weirich, T. E., Pitsch, H. and Palkovits, R. (2019). Deactivation reactions on a commercial lean NOx-trap - Effect of hydrocarbon nature, concentration and operation temperature. *Applied Catalysis A: General*, **585**, 117178.

Smits, R. H. H. and Iwasawa, Y. (1995). Reaction mechanisms for the reduction of nitric oxide by hydrocarbons on Cu-ZSM-5 and related catalysts. *Applied Catalysis B: Environmental* **6**, **3**, L201–L207.

Snow, R., Dobson, D., Hammerle, R. and Katare, S. (2007). Robustness of a LNT-SCR system to aging protocol. *SAE Paper No.* 2007-01-0469.

Song, J. H., Park, D. C., You, Y.-W., Chang, T. S., Heo, I. and Kim D. H. (2020). Lean NOx reduction by CO at low temperature over bimetallic $IrRu/Al_2O_3$ catalysts with different Ir : Ru ratios. *Catalysis Science & Technology* **10**, **7**, 2120–2136.

Song, J., Wang, Y., Walter, E. D., Washton, N. M., Mei, D., Kovarik, L., Engelhard, M. H., Prodinger, S., Wang, Y., Peden, C. H. F. and Gao, F. (2017). Toward rational design of Cu/SSZ-13 selective catalytic reduction catalysts: implications from atomic-level understanding of hydrothermal stability. *ACS Catalysis* **7**, **12**, 8214–8227.

Sreekanth, P. M. and Smirniotis, P. G. (2008). Selective reduction of NO with CO over titania supported transition metal oxide catalysts. *Catalysis Letters* **122**, **1-2**, 37–42.

Sumiya, S., He, H., Abe, A., Takezawa, N. and Yoshida, K. (1998). Formation and reactivity of isocyanate (NCO) species on Ag/Al_2O_3. *J. Chemistry Society, Faraday Trans*. **94**, **15**, 2217–2219.

Sun, J., Ge, C., Yao, X., Zou, W., Hong, X., Tang, C. and Dong, L. (2017). Influence of different impregnation modes on the properties of $CuOCeO_2/\gamma$-Al_2O_3 catalysts for NO reduction by CO. *Applied Surface Science*, **426**, 279–286.

Sun, T., Fokeme, M. D. and Ying, J. Y. (1997). Mechanistic study of NO reduction with methane over Co^{2+} modified ZSM-5 catalysts. *Catalysis Today* **33**, **1–3**, 251–261.

Takahashi, A., Fujitani, T., Nakamura, I., Katsuta, Y., Haneda, M. and Hamada, H. (2006). Excellent promoting effect of Ba addition on the catalytic activity of $Ir/WO_3–SiO_2$ for the selective reduction of NO with CO. *Chemistry Letters*, **35**, **4**, 420–421.

Takahashi, N., Shinjoh, H., Ijima, T., Suzuki, T., Yamazaki, K., Yokota, K., Suzuki H., Miyoshi, N., Matsumoto, S., Tanizawa, T., Tanaka, T., Tateishi, S.-S. and Kasahara, K. (1996). The new concept 3-way catalyst for automotive lean-burn engine: NOx storage and reduction catalyst. *Catalysis Today* **27**, **1-2**, 63–69.

Toops, T. J., Bunting, B. G., Nguyen, K. and Gopinath, A. (2007). Effect of engine-based thermal aging on surface morphology and performance of Lean NOx Traps. *Catalysis Today* **123**, **1–4**, 285–292.

Toops, T. J., Smith, D. B. and Partridge, W. P. (2005). Quantification of the in situ DRIFT spectra of Pt/K/γ-$A1_2O_3$ NOx adsorber catalysts. *Applied Catalysis B: Environmental* **58**, **3-4**, 245–254.

Tschoeke, H., Graf, A., Stein, J., Krüger, M., Schaller, J., Breuer, N. Engeljehringer, K. and Schindler, W. (2010). *Diesel Engine Exhaust Emissions. In: Mollenhauer K., Tschöke H. (eds) Handbook of Diesel Engines*. Springer, Berlin, Heidelberg, 417–485.

Urrutxua, M., Pereda-Ayo, B., De-La-Torre, U. and González-Velasco, J. R. (2019). Evaluation of Cu/SAPO-34 catalysts prepared by solid-state and liquid ion-exchange methods for NOx removal by NH_3-SCR. *ACS Omega* **4**, **12**, 14699–14713.

Vaclavik, M., Novak, V., Brezina, J., Koci, P., Gregori, G. and Thompsett, D. (2016). Effect of diffusion limitation on the performance of multi-layer oxidation and lean NOx trap catalysts. *Catalysis Today* **273**, 112–120.

Wang, A., Ma, L., Cong, Y., Zhang, T. and Liang, D. (2003). Unique properties of Ir/ZSM-5 catalyst for NO reduction with CO in the presence of excess oxygen. *Applied Catalysis B: Environmental* **40**, **4**, 319–329.

Wang, A., Wang, Y., Walter, E. D., Washton, N. M., Guo, Y., Lu, G., Peden, C. H. F. and Gao, F. (2019a). NH_3-SCR on Cu, Fe and Cu + Fe exchanged beta and SSZ-13 catalysts: Hydrothermal aging and propylene poisoning

effects. *Catalysis Today* **320**, 91–99.

Wang, J., Ji, Y., Easterling, V., Croker, M., Dearth, M. and McCabe, R. W. (2011). The effect of regeneration conditions on the selectivity of NOx reduction in a fully formulated lean NOx trap catalyst. *Catalysis Today* **175**, **1**, 83–92.

Wang, J., Peng, Z., Qiao, H., Han, L., Bao, W., Chang, L., Feng, G. and Liu, W. (2014). Influence of aging on in situ hydrothermally synthesized Cu-SSZ-13 catalyst for NH_3-SCR reaction. *RSC Advances* **4**, **80**, 42403–42411.

Wang, L., Yin, C. and Yang, R. T. (2016). Selective catalytic reduction of nitric oxide with hydrogen on supported Pd: Enhancement by hydrogen spillover. *Applied Catalysis A: General*, **514**, 35–42.

Wang, X., Wang, X., Yu, H. and Wang, X. (2019b). The functions of Pt located at different positions of HZSM-5 in H_2-SCR. *Chemical Engineering J*. **355**, 470–477.

Wu, S., Li, X., Fang, X., Sun, Y., Sun, J., Zhou, M. and Zang, S. (2016). NO reduction by CO over TiO_2-Γ-Al_2O_3 supported In/Ag catalyst under lean burn conditions. *Chinese J. Catalysis* **37**, **11**, 2018–2024.

Xiong, S., Peng, Y., Wang, D., Huang, N., Zhang, Q., Yang, S., Chen, J. and Li, J. (2020). The role of the Cu dopant on a Mn_3O_4 spinel SCR catalyst: Improvement of low-temperature activity and sulfur resistance. *Chemical Engineering J*., **387**, 124090.

Xu, G., Ma, J., Wang, L., Xie, W., Liu, J., Yu, Y. and He, H. (2019). Insight into the origin of sulfur tolerance of Ag/Al_2O_3 in the H_2-C_3H_6-SCR of NOx. *Applied Catalysis B: Environmental*, **244**, 909–918.

Xu, G., Yu, Y. and He, H. (2018). Silver Valence State Determines the Water Tolerance of Ag/Al_2O_3 for the H_2–C_3H_6–SCR of NOx. *J. Physical Chemistry C* **122**, **1**, 670–680.

Xu, R., Wang, Z., Liu, N., Dai, C., Zhang, J. and Chen, B. (2020). Understanding Zn functions on hydrothermal stability in a one-pot-synthesized Cu&Zn-SSZ-13 catalyst for NH_3 selective catalytic reduction. *ACS Catalysis* **10**, **11**, 6197–6212.

Yamamoto, T., Tanaka, T., Kuma, R., Suzuki, S., Amano, F., Shimooka, Y., Kohno, Y., Funabiki, T. and Yoshida, S. (2002a). NO reduction with CO in the presence of O_2 over Al_2O_3-supported and Cu-based catalysts. *Physical Chemistry Chemical Physics* **4**, **11**, 2449–2458.

Yamamoto, T., Tanaka, T., Suzuki, S., Kuma, R., Teramura, K., Kou, Y., Funabiki, T. and Yoshida, S. (2002b). NO reduction with CO in the presence of O_2 over Cu/Al_2O_3 (3) – structural analysis of active species by means of XAFS and UV/VIS/NIR spectroscopy. *Topics Catalysis* **18**, **1-2**, 113–118.

Yan, J.-Y., Kung, H. H., Sachtler, W. M. H. and Kung, M. C. (1998). Synergistic effect in lean NOx reduction by CH_4 over Co/Al_2O_3 and H-Zeolite catalysts. *J. Catalysis* **175**, **2**, 294–301.

You, R., Meng, M., Zhang, J., Zheng, L., Hu, T. and Li, X. (2019). A noble-metal-free SCR-LNT coupled catalytic system used for high concentration NOx reduction under lean-burn condition. *Catalysis Today*, **327**, 347–356.

Yu, Y., He, H., Zhang, X. and Deng, H. (2014). A common feature of H_2-assisted HC-SCR over Ag/Al_2O_3. *Catalysis Science & Technology* **4**, **5**, 1239–1245.

Zhang, D., Wang, Y. and Yang, R. T. (2018). Chemical Liquid Deposition (CLD)-modified Fe-ZSM-5 for enhanced activity and resistance to C_3H_6 poisoning in selective catalytic reduction with NH_3 (NH_3-SCR). *Industrial & Engineering Chemistry Research* **57**, **40**, 13586–13590.

Zhang, T., Qiu, F. and Li, J. (2016). Design and synthesis of core-shell structured meso-Cu-SSZ-13@mesoporous aluminosilicate catalyst for SCR of NOx with NH_3: Enhancement of activity, hydrothermal stability and propene poisoning resistance. *Applied Catalysis B: Environmental*, **195**, 48–58.

Zhang, X., Dou, T., Wang, Y., Yang, J., Wang, X., Guo, Y., Shen, Q., Zhang, X. and Zhang, S. (2019a). Green synthesis of Cu-SSZ-13 zeolite by seed-assisted route for effective reduction of nitric oxide. *J. Cleaner Production*, **236**, 117667.

Zhang, X., Yu, Y. and He, H. (2007). Effect of hydrogen on reaction intermediates in the selective catalytic reduction of NOx by C_3H_6. *Applied Catalysis B: Environmental* **76**, **3–4**, 241–247.

Zhang, Y., You, R., Liu, D., Liu, C., Li, X., Tian, Y., Jiang, Z., Zhang, S., Huang, Y., Zha, Y. and Meng, M. (2015). Carbonates-based noble metal-free lean NOx trap catalysts MOx–K_2CO_3/$K_2Ti_8O_{17}$ (M = Ce, Fe, Cu, Co) with superior catalytic performance. *Applied Surface Science*, **357**, 2260–2276.

Zhang, Y., Zeng, H., Jia, B., Wang, Z. and Liu, Z. (2019b). Selective catalytic reduction of NOx by H_2 over Pd/TiO_2 catalyst. *Chinese J. Catalysis* **40**, **6**, 849–855.

Zhang, Y., Zhao, L., Duan, J. and Bi, S. (2020). Insights into deNOx processing over Ce-modified Cu-BTC catalysts for the CO-SCR reaction at low temperature by in situ DRIFTS. *Separation Purification Technology,* **234**, 116081.

Zhao, H., Zhao, Y., Liu, M., Li, X., Ma, Y., Yong, X., Chen, H. and Li, Y. (2019a). Phosphorus modification to improve the hydrothermal stability of a Cu-SSZ-13 catalyst for selective reduction of NOx with NH_3. *Applied Catalysis B: Environmental* **252**, 230–239.

Zhao, X., Zhang, X., Xu, Y., Wang, X. and Yu, Q. (2015). The effect of H_2O on the H_2-SCR of NOx over Pt/HZSM-5. *J. Molecular Catalysis A: Chemical*, **400**, 147–153.

Zhao, Y., Choi, B. and Kim, D. (2017). Effects of Ce and Nb additives on the de-NOx performance of SCR/CDPF system based on Cu-beta zeolite for diesel vehicles. *Chemical Engineering Science* **164**, 258–269.

Zhao, Z., Yu, R., Shi, C., Gies, H., Xiao, F.-S., De vos, D., Yokoi, T., Bao, X., Kolb, U., McGuire, R., Parvulescu, A.-N., Maurer, S., Müller, U. and Zhang, W. (2019b).

Rare-earth ion exchanged Cu-SSZ-13 zeolite from organotemplate-free synthesis with enhanced hydrothermal stability in NH_3-SCR of NOx. *Catalysis Science Technology* **9**, **1**, 241–251.